Current Medicinal Chemistry, 2021, *28*, 3287-3317

REVIEW ARTICLE

Diffuse Intrinsic Pontine Glioma (DIPG): Breakthrough and Clinical Perspective

Maria Grazia Perrone[1,*], Antonio Ruggiero[2], Antonella Centonze[1], Antonio Carrieri[1], Savina Ferorelli[1] and Antonio Scilimati[1,*]

[1]*Department of Pharmacy and Pharmaceutical Sciences, University of Bari, Via E. Orabona 4, 70125 Bari, Italy;* [2]*Pediatric Oncology Unit, Fondazione Policlinico Universitario Agostino Gemelli IRCCS, Università Cattolica del Sacro Cuore, Largo A. Gemelli 8, 00168 Rome, Italy*

Abstract: Diffuse intrinsic pontine glioma (DIPG) mainly affects children with a median age of 6-7 years old. It accounts for 10% of all pediatric tumors. Unfortunately, DIPG has a poor prognosis, and the median survival is generally less than 16-24 months independently from the treatment received. Up to now, children with DIPG are treated with focal radiotherapy alone or in combination with antitumor agents.

In the last decade, ONC201 known as dopamine receptor antagonist was uncovered, by a high throughput screening of public libraries of compounds, to be endowed with cytotoxic activity against several cancer cell lines. Efforts were made to identify the real ONC201 target, responsible for its antiproliferative effect. The hypothesized targets were the Tumor necrosis factor-Related Apoptosis-Inducing Ligand stimulation (TRAIL), two oncogenic kinases (ERK/AKT system) that target the same tumor-suppressor gene (FOXO3a), dopamine receptors (DRD2 and DRD3 subtypes) and finally the mitochondrial Caseynolitic Protease P (ClpP). ONC201 structure-activity relationship is extensively discussed in this review, together with other two classes of compounds, namely ADEPs and D9, already known for their antibiotic activity but noteworthy to be discussed and studied as potential "leads" for the development of new drugs to be used in the treatment of DIPG.

In this review, a detailed and critical description of ONC201, ADEPs, and D9 pro-apoptotic activity is made, with particular attention to the specific interactions established with its targets that also are intimately described. Pubmed published patents and clinical trial reports of the last ten years were used as the bibliographic source.

ARTICLE HISTORY

Received: March 13, 2020
Revised: July 16, 2020
Accepted: July 23, 2020

DOI:
10.2174/0929867327666200806110206

Keywords: Diffuse intrinsic pontine glioma (DIPG), ONC201, ADEPs, D9, Dopamine receptors, CHOP, TRIAL, FOXO3a, ERK/AKT system, ClpP, SAR, Clinical Trials.

1. INTRODUCTION

Diffuse intrinsic pontine glioma (DIPG) is a tumor first described in 1926 by Wilfred Harris [1]. It accounts for 10% of all pediatric brain tumors and is almost exclusively reported in children with a median age at diagnosis of 6-7 years old [2].

Children with DIPG typically present a 1-3 months history of classic clinical symptoms characterized by cranial nerve palsy, ataxia, and pyramidal tract abnormalities. Following diagnosis, the median progression-free survival is approximately 7 months with a mean survival time beyond the progression of 3 months irrespective of the treatment received [3]. Despite the adoption of aggressive therapeutic approaches, DIPG remains the leading cause of cancer-related mortality in childhood and DIPG prognosis is still poor with more than 90% of affected children dying within 18-24 months from diagnosis [2, 4].

Taking into account the tumor location within the brainstem and their infiltrative pattern, diagnosis is generally based on the clinical history and magnetic resonance imaging. Surgical partial removal or biopsy

*Address correspondence to these authors at the Department of Pharmacy and Pharmaceutical Sciences, University of Bari, Via E. Orabona 4, 70125 Bari, Italy; Tel/Fax: +390805442753/ +390805442050; E-mail: antonio.scilimati@uniba.it (A.S); Tel/Fax: +390805442747/+390805442050; E-mail: mariagrazia.perrone@uniba.it (M.G.P.)

1875-533X/21 $65.00+.00

of the tumor are not routinely performed as the results do not impact on treatment choice and survival [5].

However, in the last decade, biological features of DIPG provided new additional molecular data helpful to better classify this fatal tumor. In 2012, Schwartzentruber *et al.* identified a pathognomic and negative prognostic H3 K27M mutation present in approximatively 80% of DIPG [6]. The same mutation has been reported to be present in many thalamic and spinal cord gliomas. The last 2016 WHO central nervous system tumor classification has incorporated these histopathological findings and reclassification has defined a new entity "diffuse midline glioma H3 K27M mutant" which is histologically related to a grade IV glioma [7].

Decades of clinical attempts involving more than 200 trials evaluating different conventional cytotoxic drugs, myeloablative regimens with stem cell transplantation, targeted drugs, and studies with escalating radiation dose or using new radio-sensitizing agents, have failed to improve the overall survival of children with DIPG [8, 9]. The current standard treatment is still based on the non-curative focal radiotherapy often resulting only in a transient stabilization of the disease with a marginal influence on the fatal clinical course [10].

The scientific interest in DIPG surged in recent years (Fig. **1A** and **1B**). In the timeframe 1989-2020, 560 papers were published, most of them appeared since 2010 (more than 10 papers/year) [11].

By using approximately 2000 small molecules of the Diversity Set II of the National Cancer Institute chemical library, in a phenotypic screening for p53-independent inducers of TRAIL-mediated apoptosis, the compound **ONC201** (previously named **TIC10**) was identified [12]. Then, several studies investigated its mechanism of action to ascertain the corresponding biological target (Fig. **1C**). Soon after, **ONC201** was proposed as a treatment of high-grade gliomas, including DIPG for its ability to cross the brain-blood barrier [13, 14].

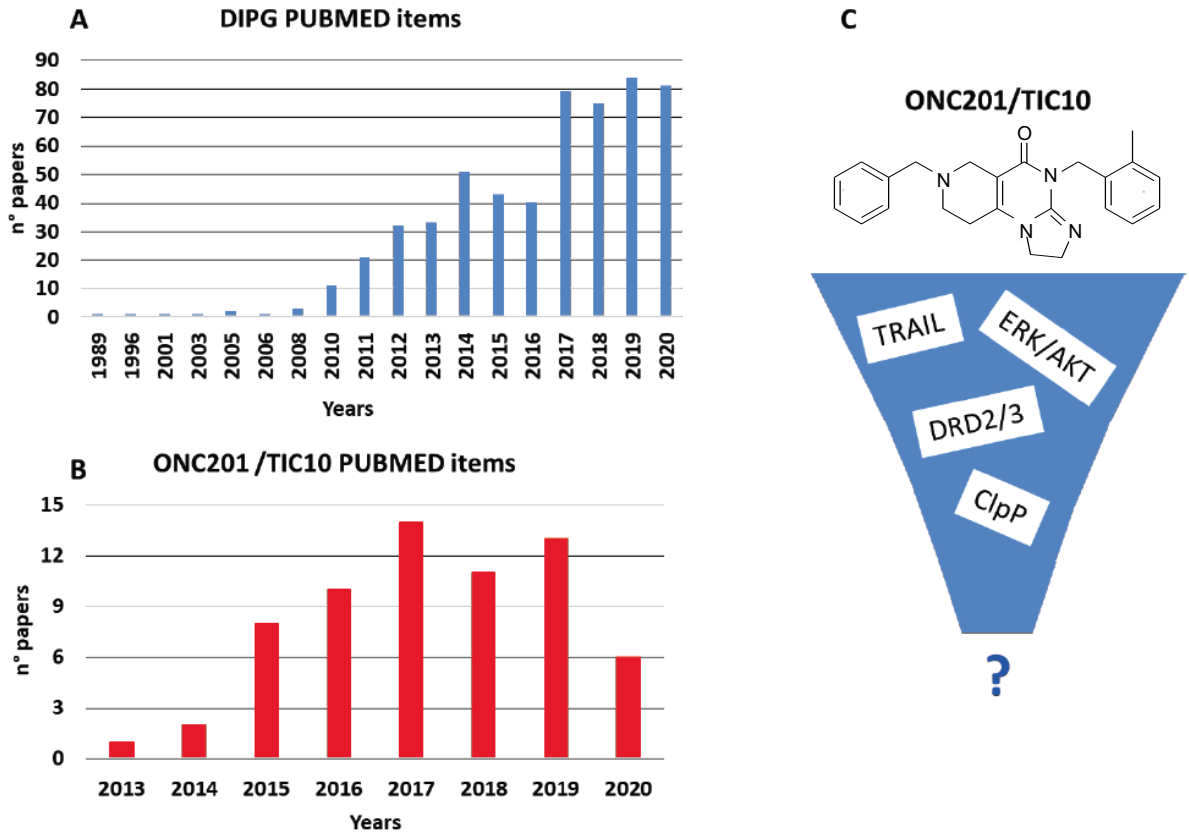

Fig. (1). A. Papers dealing with DIPG published in PubMed in years 1989-2020 (the year 2020 paper number is partial because references were checked within March 2020); **B**. Papers dealing with ONC201 for the treatment of DIPG in years 2013-2020; **C**. ONC201/TIC10 hypothesized mechanism of action: TRAIL (Tumor necrosis factor-Related Apoptosis-Inducing Ligand stimulation) upregulation, ERK/AKT system inactivation, dopamine receptors (DRD2 and DRD3 subtypes) antagonism, ClpP (Caseynolitic Protease P). *(A higher resolution / colour version of this figure is available in the electronic copy of the article).*

2. DEATH RECEPTORS AND TUMOR NECROSIS FACTOR-RELATED APOPTOSIS-INDUCING LIGAND STIMULATION (TRAIL)

Since **ONC201** was been identified from TRAIL-mediated apoptosis inducer screening, the first proven mechanism of its action was the stimulation of TRAIL production in tumor cells [15]. TRAIL (Apo-2 ligand, CD253, or TNF-SF10), belonging to the TNF superfamily cytokines, induces apoptosis/survival according to the receptor to which it binds [16].

Five TRAIL receptors are known: two membrane-bound decoy receptors DcR1and DcR2, two death receptors DR4 and DR5, and one osteoprotegerin (OPG) receptor [16, 17].

- **DcR1** (TNFRSF10c, TRAILR3) and **DcR2** (TNFRSF10d, TRAILR4) are unable to activate apoptotic signaling and inhibit TRAIL signaling. DcR1 functions as a TRAIL-neutralizing decoy receptor and is devoid of signaling capabilities. DcR2 contains a cytoplasmic domain that lacks a functional death domain; therefore, TRAIL binding to DcR2 activates NF-κB and leads to the transcription of genes that promote cell survival and resistance to apoptosis.
- **DR4** (TNFRSF10a, TRAILR1) and **DR5** (TNFRSF10b, TRAILR2) are both involved in apoptotic pathways. TRAIL typically binds to DR4 or DR5 and induces caspase-8-dependent apoptosis through a functional cytoplasmic death domain. TRAIL signaling leads to cell death by both extrinsic (damage caused by external signal: TNF and FAS-ligand) and intrinsic (intracellular damages: oxidative stress, DNA-damage p53 mediated) pathways. The intrinsic pathway passes through mitochondrial permeabilization and releasing of pro-apoptotic factors as caspase cascade activation inducers. TRAIL binding to DR4 or DR5 causes receptor clustering and trimerization. Intracellular adaptor protein Fas-associated protein with death domain (FADD) is recruited to the death domain of the TRAIL receptor. Initiator caspase-8 is recruited to the death-inducing signaling complex (DISC) and interacts with FADD through their death effector domains. DISC activation of caspase-8 leads to caspase cascade activation where downstream effector caspase-3 is activated and cleaves protein targets that culminate in cell death. Additionally, caspase-8 can cleave the Bcl-2 related protein Bid. Truncated Bid (tBid) translocates into the mitochondria, where it causes the release of cytochrome c and the formation of the Apaf-1 containing apoptosome, and subsequent caspase-9 activation. Activated caspase-9 can then activate effector caspase-3 resulting in cell death (Fig. **2**) [18].

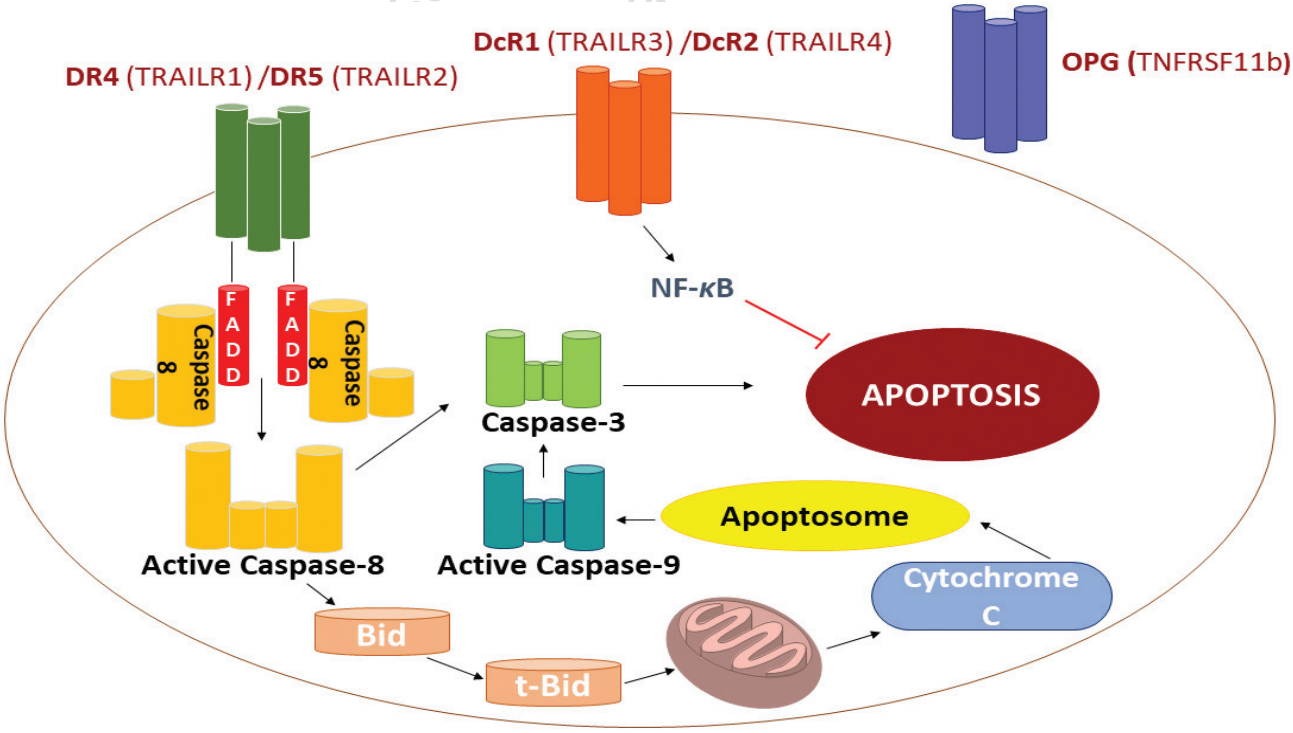

Fig. (2). Summary of apoptotic events induced by TRAIL. *(A higher resolution / colour version of this figure is available in the electronic copy of the article).*

- The fifth TRAIL-binding receptor is osteoprotegerin (**TNFRSF11b**), a soluble protein that likely is a decoy/inhibitor by sequestering TRAIL extracellularly [17].

Hence, TRAIL seems a crucial target endowed with anti-tumor activity, and specifically, its up-regulation could be a reasonable strategy to induce apoptosis of tumor cells.

ONC201 powerfully and selectively induces cell growth block and apoptosis in several tumors, with limited or no toxicity in normal cells [19]. **ONC201** also causes an "integrated stress response" (ISR), a eukaryotic cell adaptive pathway due to different stimuli, which is decisive for **ONC201** pro-apoptotic effects. Indeed, ISR activates Activating transcription factor 4 (ATF4) and C/EBP homologous protein (CHOP) transcription factors, involved in the TRAIL DR5 receptor up-regulation that promotes apoptosis [20].

As mentioned above, **ONC201** induces TRAIL in some but not in all cell types [21]. Specifically, TRAIL was not increased in breast cancer cell lines even though **ONC201** strongly reduced cell viability [22]. **ONC201** was also effective against TRAIL-resistant breast cancer cells and hematological malignancies independently of TRAIL [23, 24].

These findings led to look for alternative **ONC201** mechanisms of action to justify its antitumoral activity also in those cell lines in which apoptotic effects were observed without the TRAIL induction [20].

3. Akt/ERK SYSTEM

Afterward, the **ONC201** antitumoral effect was linked to the inhibition of Akt/ERK activity, two oncogenic kinases that target the same tumor-suppressor gene, FOXO3a [25, 26].

Forkhead box proteins (FOX) are a family of highly conserved transcription factors, characterized by a "helix-turn-helix" DNA-binding (FKH) formed by a winged fork-shaped structure composed of three α helices and two-ring or "wing" domains. The bifurcated domain is also known as a winged-helix due to the apparent butterfly shape of the loops in the protein structure of the domain [27].

Based on the homology of the amino acid sequence, more than 2000 members belonging to this family of transcription factors are currently known. Various FOXs differ in all domains except for forked domain that binds DNA, and consists of about 100 amino acid residues. For that reason, FOXs have very different binding specificities and consequently, different cellular effects. They are classified in different sub-families: FOXM, FOXK, FOXA, and FOXO [28].

FOXO is an ubiquitary transcription factor that regulates different developmental processes, energy metabolism, and carcinogenesis in many tissues. Deregulation of the FOXO functions causes an uncontrolled cellular proliferation and an accumulation of DNA damage, which causes carcinogenesis. In mammals, four isoforms are recognizable: FOXO1, FOXO3a, FOXO4, and FOXO6, known to be regulated by phosphoinositol-3-kinase (PI3K). Particularly, FOXO3a phosphorylation by PI3K/Akt (phosphoinositide 3-kinase/Akt) is the most studied one (Fig. **3**) [29].

FOXO3a is approximately a 71 kDa protein and its structure is conserved across different species. FOXO3a gene is located on chromosome 6q21 and plays a vital role in regulating different cellular processes targeting both the expression and effects of effector genes. It has five domains (Fig. **3**). The forked domain is mainly responsible for direct interaction between FOXO3a and DNA and favors its interaction with the estrogen receptor α (ERα) and p53. NLS domain is necessary for FOXO3a translocation from the cytoplasm to the nucleus and mediates the FOXO3a release from the nucleus. The C-terminal TAD domain is vital for the transactivation of genes encoding FOXO3a [27]. FOXO3a is a transcription factor involved in different physiological and pathological events. It promotes the transcription of target genes involved in apoptosis, proliferation, cell cycle progression, DNA survival, and damage. FOXO3a responds to various cellular stimuli, such as UV radiation and oxidative stress [30]. It is also associated with longevity and regulation of auto-phage processes in muscle and cancer cells [27]. FOXO3a Akt-dependent phosphorylation improves the interaction of FOXO3a with the 14-3-3 protein and promotes FOXO3a translocation nucleus-cytoplasm, thereby blocking FOXO3a transcriptional activity [31]. FOXO3a phosphorylation by ERK induces a conformational modification and promotes the interaction between FOXO3a and ubiquitin E3 ligase MDM2, thereby leading to ubiquitination of FOXO3a and proteasomal degradation [32]. In the nucleus, FOXO3a is acetylated by p300 and CREB-binding protein (CBP) and is deacetylated by SIRT1. SIRT1-mediated deacetylation changes FOXO3a binding affinity for DNA, while deacetylation by SIRT2 increases its binding activity for DNA [33].

FOXO3a methylation, by arginine methyltransferase 1 (CARM1) associated with its co-activator, is

Fig. (3). FOXO3a has five domains: a winged fork domain (FKH), DNA helix-helix-binding, two nuclear localization sequences (NLS), a nuclear export sequence (NES) and a C-terminal transactivation domain (TAD). *(A higher resolution / colour version of this figure is available in the electronic copy of the article).*

necessary for FOXO3a activation in the nucleus. Particularly, FOXO3a Lys270 methylation reduces the ability to bind DNA and also reduces FOXO3a-mediated apoptosis (Fig. **4**) [27]. By inhibiting kinases Akt or ERK, FOXO3a remains in the nucleus and this determines the progression of the apoptotic process of the tumor cells. In fact, by binding to DNA, the expression of pro-apoptotic genes, including TRAIL is induced. Only if the kinases are inhibited, FOXO3a is not phosphorylated and therefore cannot move into the cytoplasm (inactive FOXO3a) but is forced to remain in the nucleus (active FOXO3a) [34].

4. DOPAMINE RECEPTOR (DR)D2, (DR)D3 AND ONC201

Although TRAIL and Akt/ERK can certainly explain the pro-apoptotic activity of **ONC201**, they did not seem its direct target. A novel paradigm (BANDIT) combining big-data from clinical, genomic, chemical, and structural datasets within a Bayesian machine-learning framework to predict the targets of small molecules was developed [35]. It was found that the most likely targets of **ONC201** were two G-protein coupled receptors (GPCRs), specifically dopamine receptors - mainly DRD2 - and alpha-adrenergic receptors [36]. DRD2 is overexpressed in many types of cancers, including high-grade gliomas, and its expression is associated with a poor prognosis [9, 37]. The use of dopaminergic drugs for the treatment of schizophrenia and Parkinson's disease is associated with reduced cancer risk [38]. As a GPCR, DRD2 controls mitogenic and other signaling pathways that are related to tumorigenesis, cell proliferation, and metastatic dissemination. Selective DRD2 antagonism causes inactivation of MAPK signaling and induces tumor cell death in preclinical models of high-grade gliomas and other malignancies [35, 39]. The dopamine receptor family consists of 5 members, categorized as D1-like and D2-like subfamilies based on their coupling to different GPCR-alpha proteins that cause opposing downstream signalings [37].

ONC201 was found to be a selective antagonist of DRD2 and DRD3 [9, 35] with a K_i of 3 μM [36].

The hypothesis that DRD2 ligands may be used as cancer chemotherapy had a big appeal due to a large number of known, approved, and under investigation drugs of this class that could be repurposed.

Preclinical data have shown that H3 K27M-mutant gliomas are characterized by an elevated DRD2 expression and enhanced sensitivity to **ONC201** (Figs. **5** and **6**) [40].

In particular, 625 mg every 3 weeks was the recommended phase II dose of **ONC201** for H3 K27M–mutant glioma patients [41]. Further studies demonstrated that a weekly administration of **ONC201** is equivalent in terms of safety and enhanced immunostimulatory activity [42]. Furthermore, phase I e phase II clinical trials adopting **ONC201** as a single agent in children and adults with high-grade gliomas and H3 K27M–mutant gliomas suggest favorable activity and tolerability profile [43-45].

DRD2 antagonists play their anticancer activity as cell cytotoxic agents when used in large doses since their receptor affinity is very low (all tested drugs have an affinity of 0.12-430 nM for DRD2 and 0.3-340 nM for DRD3) and this should be taken into account, also for CNS adverse effects [46].

It is noteworthy, that a compound with low activity and/or selectivity in cell culture, may not achieve meaningful concentration levels in circulating blood, and hence to be an anticancer agent. In other words, additional studies are needed to further clarify the use of ligands targeting D2-like dopamine receptors in cancer chemotherapy.

ONC201 exerts its antagonism by orthosteric interactions with the binding pocket defined by the side chains of helices III, V, and VI interacting with Cys118, Thr119, Ser197, Phe198, Phe382, Phe390, and Trp386 forming a subpocket below the orthosteric site (Fig. **6**) [47]. Specifically, **ONC201** shows a relatively slow association and rapid dissociation with DRD2, behavior that is not generally associated with extrapyramidal side effects [48].

5. CASEYNOLITIC PROTEASE P (ClpP)

To the best of our knowledge, the anticancer activity of **ONC201** can not be attributed to the only dopaminergic antagonism that has to be still explored and

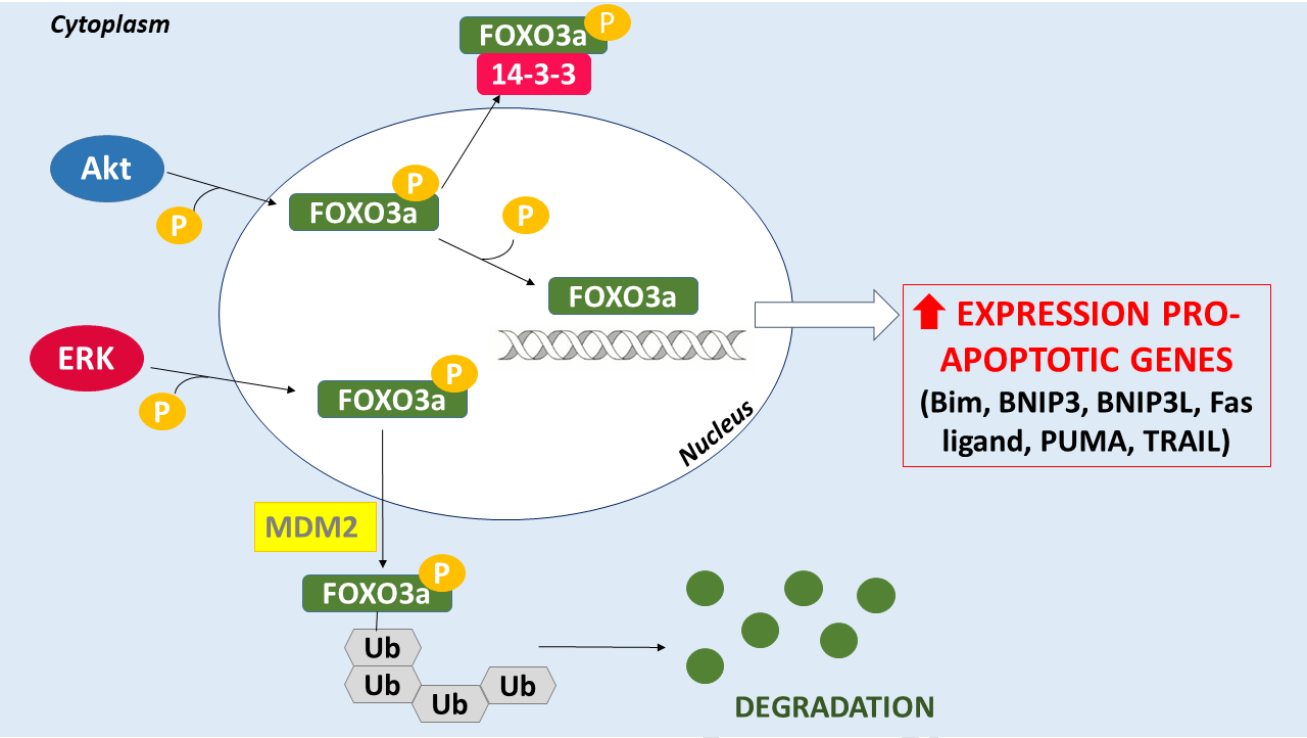

Fig. (4). FOXO3a schematic interactions inside/outside the nucleus. *(A higher resolution / colour version of this figure is available in the electronic copy of the article).*

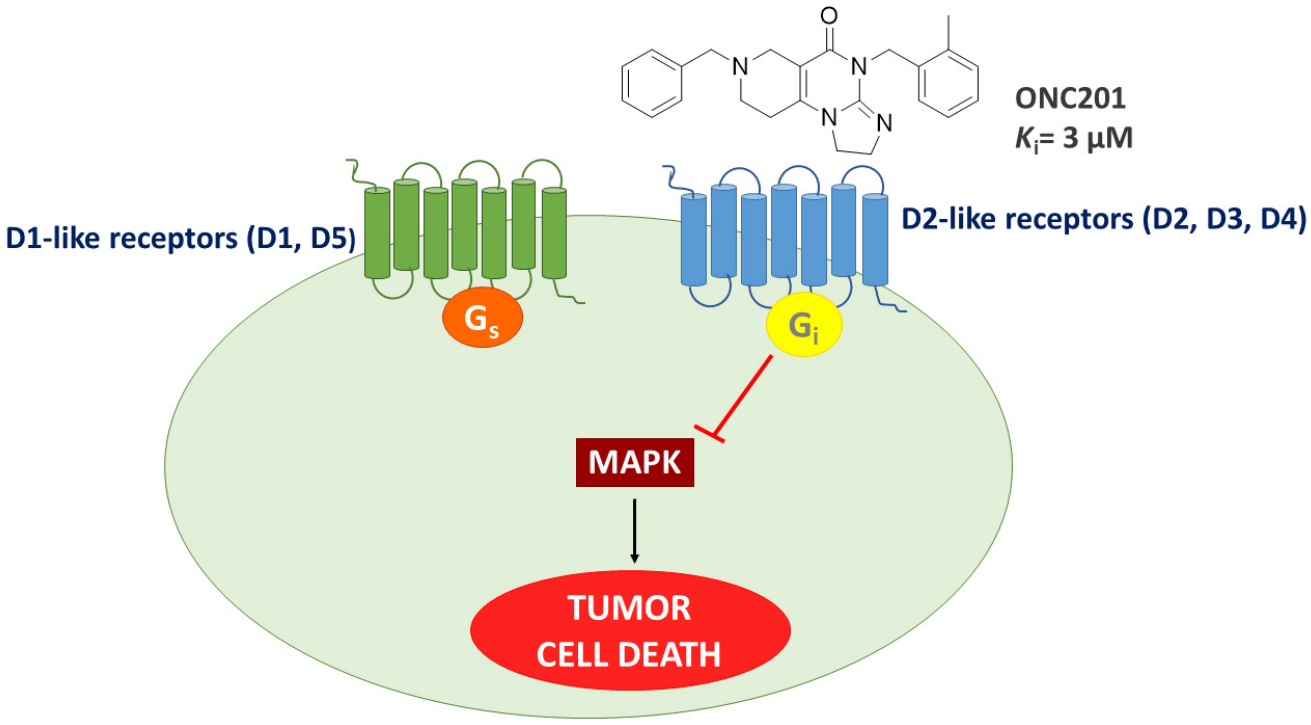

Fig. (5). ONC201 antagonism of dopamine receptors D2 and D3. *(A higher resolution / colour version of this figure is available in the electronic copy of the article).*

verified. **ONC201** would have another direct target. In fact, in May 2019, the diffractometric characterization (X-rays) of the complex between human mitochondria type C serin-proteases (ClpP) caseinolytic and **ONC201** (PDB ID 6DL7) led to identifying ClpP as its true biological target [49, 50].

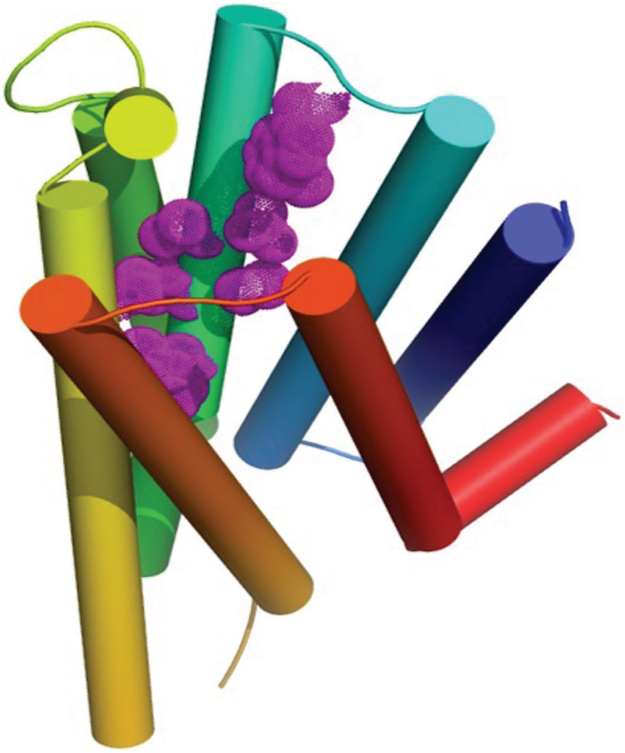

Fig. (6). Representation of the transmembrane region of DRD2. Residues comprising the orthosteric binding site are depicted in dots. *(A higher resolution / colour version of this figure is available in the electronic copy of the article).*

Caseynolitic Protease P (ClpP) is a serine protease located in the mitochondrial matrix. It is involved in the maintenance of mitochondrial proteome, in turn, obtained through different molecular mechanisms. One of these mechanisms employs molecular chaperones and proteases. The former plays an important role in the correct folding of mitochondrial proteins, the latter is involved in the elimination of damaged and/or misfolded proteins. Specifically, ClpP catalyzes substrate peptide bond hydrolysis through Ser-His-Asp catalytic triad. In mitochondria ClpP intimately interacts with ClpX, an AAA+ proteins unfoldase, responsible for proteins unfolding. AAA+ is an ATPase associated with different cellular activities, which use highly conserved AAA+ domain to bind ATP and induce hydrolysis (Fig. **7**). The complex ClpP:ClpX is ClpXP (Fig. **8**) [51].

ClpX and ClpP are differently expressed in different tissues. ClpX is strongly expressed in the skeletal and heart muscles, but less in liver, brain, placenta, lungs, kidneys, and pancreas. ClpP is found to a high extent in skeletal muscles, at intermediate levels in the heart, liver, and pancreas, and low levels in brain, placenta, lungs, and kidney.

ClpXP complex is constituted by 14 ClpP subunits, organized in two heptameric rings forming a cylinder, which are closed at each end by six ClpX subunits forming the hexameric ring (Fig. **8**).

The catalytic triad (Ser153, His178, and Asp227) is located inside the ClpP cylinder to prevent unspecific proteolytic activities, while ClpX serves as the gatekeeper recognizing only specific proteins and targets to be degraded. The interactions between ClpX and ClpP are stabilized by strong dynamic interactions between the ATPase IGF loops with the hydrophobic pockets formed by neighboring ClpP subunits at the ClpX-ClpP interface. IGF-motif loops project from the hexameric ring of ClpX and are required for docking with the self-compartmentalized ClpP peptidase, which consists of heptameric rings stacked back-to-back [52].

The degradation of a substrate protein by ClpXP occurs in a coordinated and gradual manner. Firstly, the protein substrate is recognized and bound by ClpX, then it is unfolded by ClpX in an ATP-dependent manner to be threaded through the axial pore of ClpX. The unfolded substrate translocates through ClpP lumen and is degraded into small peptides after ClpP's proteolytic residues exposition. Degraded peptides are expelled through the side pores of ClpP. At this point,

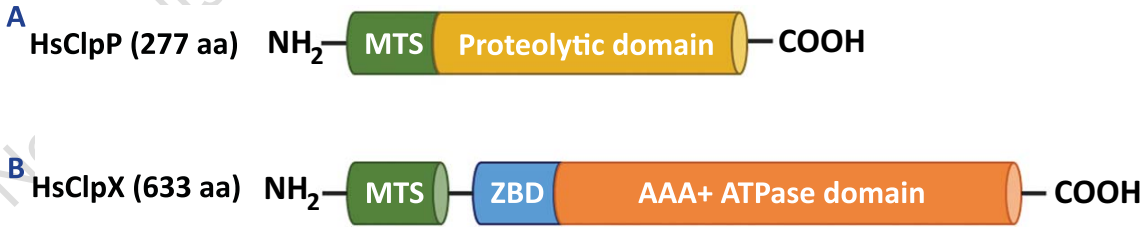

Fig. (7). ClpX and ClpP are encoded by two different nuclear genes, ClpX on chromosome 15 and ClpP on chromosome 19. **A.** HsClpP (human ClpP) is 277 amino acid residues in length and consists almost entirely of the serine protease domain. An MTS is positioned at the N-terminus of HsClpP for mitochondrial translocation. **B.** HsClpX (human ClpX) is 633 amino acid residues in length and consists primarily of the AAA+ domain preceded by a zinc-binding domain (ZBD) for substrate protein recognition. At its N-terminus, there is a mitochondrial targeting sequence (MTS), required for its translocation into the mitochondrial matrix [51]. *(A higher resolution / colour version of this figure is available in the electronic copy of the article).*

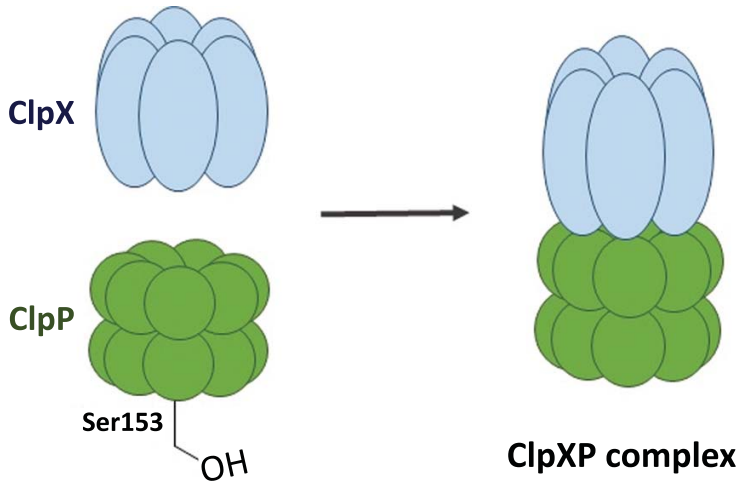

Fig. (8). Structure of the ClpXP complex. *(A higher resolution / colour version of this figure is available in the electronic copy of the article).*

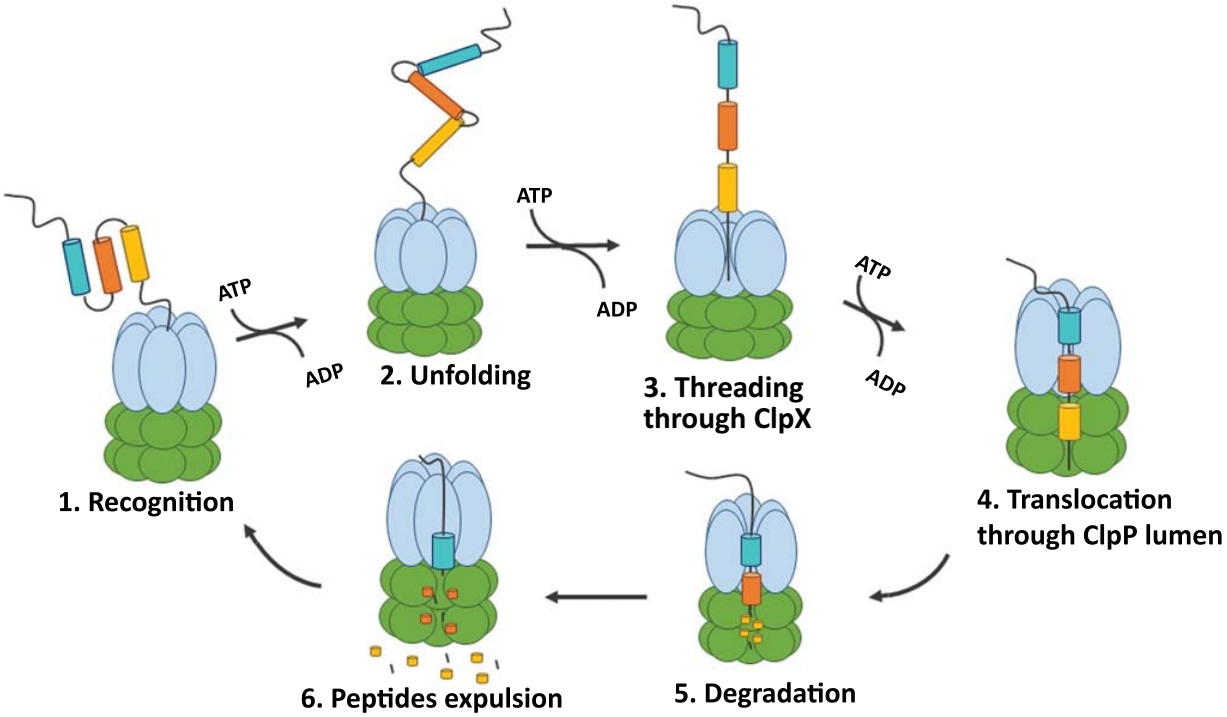

Fig. (9). Degradation cycle of a protein by ClpXP. *(A higher resolution / colour version of this figure is available in the electronic copy of the article).*

ClpXP is regenerated and can start a new cycle (Fig. **9**) [51].

The primary function of ClpXP is to facilitate the turnover of specific misfolded proteins, thus preventing their accumulation that can cause impairment of normal cellular function. The ClpXP expression, in fact, increases during a mitochondrial unfolded protein response (UPR^{mt}) upon the accumulation of misfolded mitochondrial proteins, and the respiratory deficiency caused by mitochondrial DNA (mtDNA) mutations.

Besides protein quality control, ClpXP also regulates multiple biological pathways, such as heme biosynthesis, mitophagy, and mitochondrial translation. The exact function of ClpP in cancer pathology is not well understood, although it has been observed that its expression is generally upregulated in solid tumors of multiple organs or tissues, such as lung, stomach, liver, thyroid, bladder, breast, ovary, prostate, testis and CNS. ClpP expression also increases significantly in acute myeloid leukemia [51, 53].

Recent studies suggest the involvement of ClpP in the proliferation and metastasis of specific types of cancer [54]. For example, levels of proliferation and colony formation of prostate cancer cells PC3 decrease significantly when ClpP expression is inhibited. In contrast, depleted ClpP expression has minimal effects on breast cancer cell MCF7 proliferation. This means that ClpP involvement in cancer depends on the cellular type. Based on current experimental evidence and clinical data, the ClpP expression increase does not seem to directly contribute to oncogenesis but is essential for the proliferation and metastasis of some cancer types [55].

Chemical modulators of ClpP activity are compounds originally designed as potential antibiotics against various bacterial species and other pathogenic organisms (*e.g., Plasmodium falciparum*, the causative agent of malaria) were found to be chemical modulators (inhibitors and activators) of ClpP activity. They are potential antitumoral compounds as they modulate ClpP proteolytic activity [56].

6. INHIBITORS OF ClpP ACTIVITY

The inhibitors of ClpP activity are used in those tumors where proliferation depends on the protease. Generally, they covalently modify the 14 catalytic Ser153 residues located within its lumen then disabling tetradecamer ClpP activity [51].

ClpP inhibitors can be grouped into two chemical classes:

- **β-lactones**, such as A2-32-01. They were developed as potential antibiotics to treat Staphylococcus aureus infection [57]. They covalently modify the catalytic Ser153 *via* one of the two possible reactions **a** or **b** in Fig. (**10**);

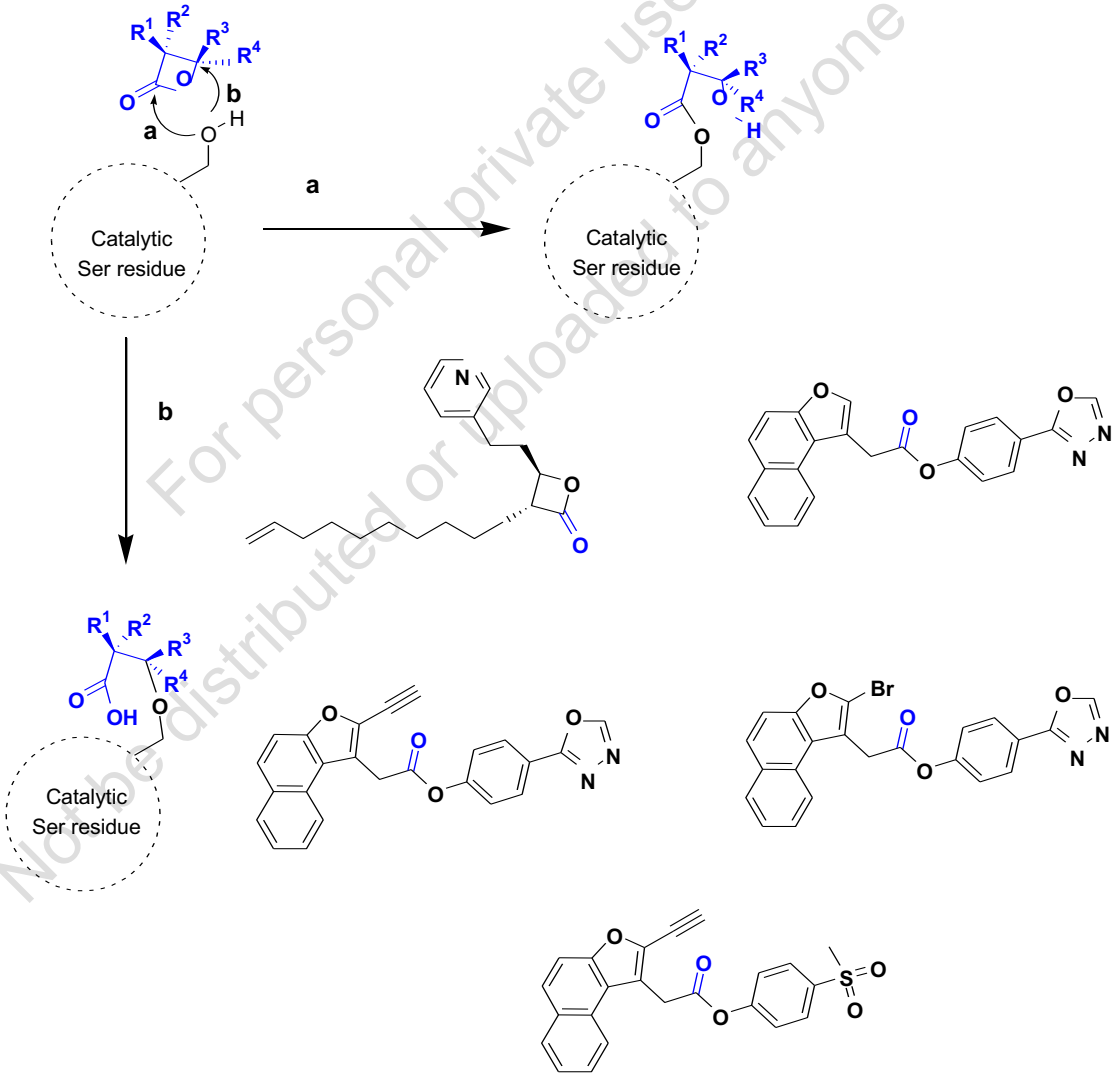

Fig. (10). ClpP Ser153 hydroxyl group-mediated reactions (**a**, **b**) by ClpP inhibitors.

- **substituted phenyl esters** (AV-167, TG42, TG43, TG53). Their mechanism of action is based on the nucleophilic attack on drug ester carbonyl with the assistance of the catalytic Ser hydroxyl group of ClpP, with consequent esterification of serine and formation of phenol (Fig. **10**). AV-167 is also active against bacterial ClpP, unlike its analogs (TG42, TG43, TG53) which are selective for human ClpP (Fig. **10**) [59].

7. ACTIVATORS OF ClpP ACTIVITY

The mechanism of action of ClpP activators is based on disruption of the ClpXP complex, by physically displacing ClpX from ClpP while keeping ClpP in its activated state (Fig. **11**). ClpP activators comprise acyldepsipeptides (*i.e.,* **ADEP4**), oxadiazoncarboxyamides (*i.e.,* **D9**) and imipridones (*i.e.,* **ONC201**).

7.1. Acyldepsipeptides (ADEPS) and Structure-activity Relationships (SAR) Studies

ADEPs are antibiotics discovered in 2005 (Table **1**) [58]. They bind the hydrophobic pockets of ClpP, which normally dock the IGF loop of ClpX. This binding disrupts the interaction between ClpP and ClpX, leading to the rapid dissociation of the ClpXP complex. Furthermore, the binding of an ADEP induces structural effects in ClpP that simulate the ClpX-ClpP interaction and forces the protease to maintain its activated state, which is characterized by structuring its axial loop and widening its axial pore that allows unrestricted access of peptides, molten globules, and loops in folded proteins to ClpP proteolytic chamber, resulting in their dysregulated degradation. ADEP-28 and ADEP-41 are known to induce cytotoxicity in T-REx HEK293 cells with sub-micromolar values of IC_{50}. These compounds show cytotoxic activity on both bacterial and human cells.

ADEPs are natural products proven to be ClpP activator. Indeed, ClpP plays an essential role in the virulence of pathogenic bacteria during host infection. ADEPs dysregulate the function of bacterial ClpXP complexes by physically displacing ClpX from ClpP but keeping ClpP in its activated state. The representative members of ADEP antibiotics are A54556A (also denoted as ADEP1) and A54556B (Table **1**) [59].

The structure-activity relationship (SAR) studies showed that replacement of *N*-methylalanine residue in the macrocycle core with a rigid pipecolate moiety lowers the entropic cost of ClpP binding. Therefore, the chemical stability and bioavailability of the compounds could be further enhanced by substituting the polyunsaturated side chain with a heptenoyl moiety and by replacement of phenylalanine in its side chain with 3,5-difluorophenylalanine. Consequently, the optimized derivative ADEP4 exhibited more chemical stability.

Hence, conformational flexibility of the core structure of ADEP-peptidolactone strongly affects ClpP binding. Replacing amino acids in the ADEP macrocycle with conformationally constrained residues, such as 4-methylpipecolate [60] and allo-threonine (**ADEP B315**), could further improve their antibacterial activity. *N*-Acylphenylalanine moiety is both necessary and

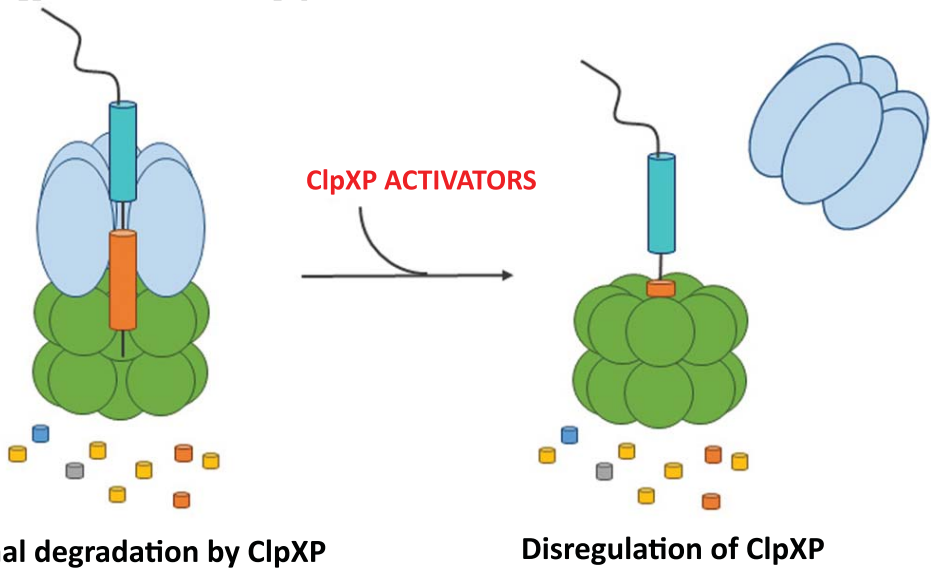

Fig. (11). Mechanism of action of ClpP activators. *(A higher resolution / colour version of this figure is available in the electronic copy of the article).*

Table 1. ADEP structures.

Structure	Compound	R	R^1	R^2	R^3
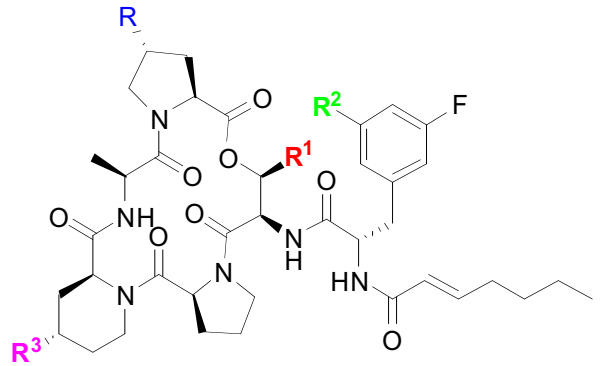	**ADEP 4**	CH_3	H	F	H
	ADEP B315	H	CH_3	F	CH_3
	Goodraid	CH_3	CH_3	F	H
	ADEP28 (socha)	H	CH_3	F	CH_3
	ADEP 41	H	CH_3	F	H
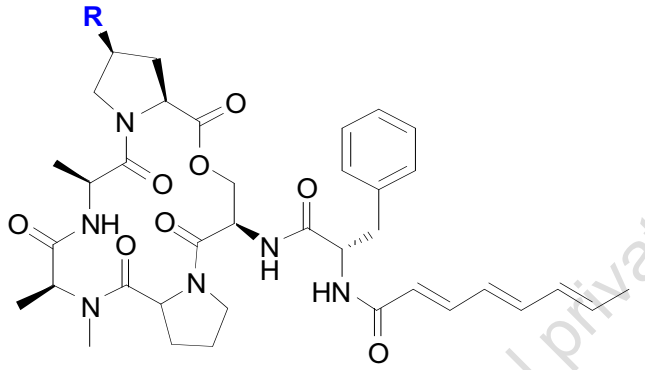	**A54556A (ADEP1)**	CH_3	-	-	-
	A54556B	H	-	-	-

sufficient for ClpP over-activation and ensures antibacterial activity. Analogs of ADEPs that specifically target human ClpP have been recently identified [55]. Notably, these compounds induce apoptotic cell death in immortalized human cancer cell lines with high potency. At first, ADEPs bind noncovalently hydrophobic pockets between neighboring ClpP subunits that normally accommodate the docking of ClpX IGF loops. ADEPs outcompetes the IGF loops of ClpX for binding to ClpP because they have a higher affinity for ClpP than ClpX. Thus, the binding of ADEPs disrupts the binding of ClpX, leading to the rapid dissociation of the ClpXP complex and hence to its inactivity. Recently, two ADEPs analogs (**ADEP-28** and **ADEP-41**) were reported [55]. They show high specificity for HsClpP and activate both the peptidase and protease activities of HsClpP with great potency.

7.2. Oxadiazoncarboxyamides and Structure-Activity Relationships (SAR) Studies

D9, as ADEPs induce dysregulated activation of ClpP, belongs to this class (Fig. **12**, Table **2**). The noncovalent binding of these compounds induces ClpP activation by the expansion of the protease axial pore, while axial loop formation was not observed [61]. They find space into the hydrophobic pockets. Importantly, **D9** showed species specificity as it preferentially activates the proteolytic activity of HsClpP, while having minimal effects on ClpP of bacterial origin.

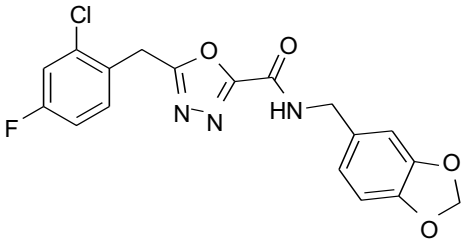

Fig. (12). Chemical structure of **D9**.

D9 is a potent and selective activator of human ClpP (HsClpP). It binds the hydrophobic pockets formed between neighboring HsClpP subunits, as for the ADEPs. These pockets are crucial for the interaction between HsClpP and HsClpX so that **D9** is considered as a chaperone ClpX mimic, in a similar way to ADEPs. Binding of **D9** stabilizes the active oligomeric state of HsClpP by widening of the protease axial pore. The selectivity of **D9** for HsClpP is due to its unique

Table 2. Examples of oxadiazoncarboxyamides.

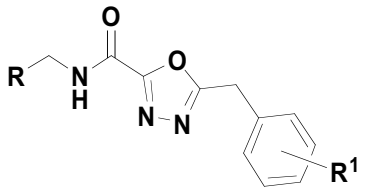

Compound	R	R^1
D9	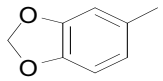	2-chloro-4-fluoro
1		2,4-dichloro
2		2,4-difluoro
3		2-chloro
4		3,5-difluoro
5		3-chloro
6		H
7		2-chloro-5-fluoro
8		3-fluoro
9		4-chloro
10		3,5-dioxane
11	-	4-methyl
12	-	3,4-dimethoxy
13	-	3,4,5-trimethoxy
14	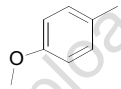	2-chloro-4-fluoro
15	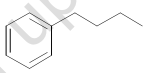	
16	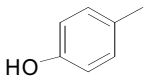	
17		
18	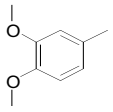	
19	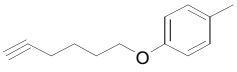	
20	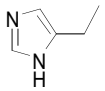	
21	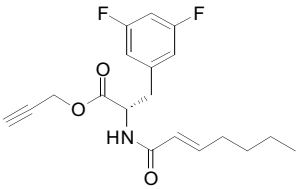	

structural composition. **D9** SAR suggests that both the halogenated benzyl and benzodioxole moiety are necessary for productive binding.

As for the benzyl moiety, the exchange of fluorine with a chlorine atom (or *vice versa*) (**1** and **2**) leads to a slightly reduced peptidase activation, while switching the two fluorine atoms to a 3,5-position (**4**) further decreased the activity 2,5-Positions occupied by chlorine and fluorine produced **7** with no activity. Derivatives with only one halogen atom reduced the activation. Both an unsubstituted benzyl group and a benzyl group bearing electron-donating methoxy (**12, 13**), methylenedioxy (**10**), and methyl (**11**) groups showed no activating effect. From these results, it is possible to deduce that halogen substitutions at the benzyl moiety are essential to boost HsClpP activity. By changing the benzodioxole moiety, it was observed that a change to a methoxy-substituted benzyl (**14**) and extension of the carbon-based linker (**15**) was tolerated, however, the introduction of hydroxy (**16**), alkyl chain (**17**), dimethoxy (**18**), alkyne (**19**), or imidazole (**20**) groups either reduced or abolished the activity.

The benzyl moiety is localized in the same hydrophobic pocket as exploited by the phenylalanine moiety of ADEPs. The hydrophobic pocket of wild-type HsClpP consists of a set of aromatic residues (Tyr118, Tyr138, Trp146), which coordinate the substituted benzyl, probably *via* π-stacking interactions triggered by electronic effects of the halogens.

Furthermore, Trp146 is a residue characteristic of HsClpP, which likely serves as a selectivity filter.

7.3. Imipridones

Imipridones including **ONC201** and its analogs (Fig. **13**) disrupt the ClpXP complex through the same mechanism of ADEP and **D9**: binding the hydrophobic pockets formed between neighboring ClpP subunits induces widening of its axial pore with consequent destruction of both mitochondrial proteins and mitochondrial respiratory chain complexes I and II subunits, in turn, determining the loss of cellular respiratory function [50].

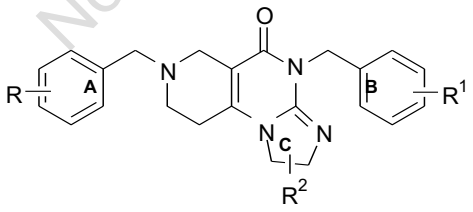

Fig. (13). Chemical structure of ONC201(R = R^1 = R^2 = H) and its analogs.

8. ONC201 PHARMACOKINETICS

ONC201 pharmacokinetics profile was determined in mice, rats, dogs, and is currently being determined in children and adults [19]. Its exposure in beagle dogs following oral gavage dosing at 4.2-120 mg/kg, was dose-dependent and increased with greater **ONC201** dose levels [21]. Exposure to **ONC201** was slightly higher in the female dogs relative to the male dogs. The terminal half-life ranged from 4.6 to 7.8 hours. In rats, exposure to **ONC201** was dose-dependent and approximately dose-proportional [21], slightly greater in female rats after a single oral gavage dose. The terminal half-life ranged from 2.3 to 8.4 hours. The volume of distribution was large, ranging from ~49 to ~103 L/kg, suggesting that **ONC201** is widely distributed. The half-life of **ONC201** in mice is ~6 hours with intravenous administration as measured by the HPLCUV assay [62]. The pharmacokinetics of the single agent **ONC201**, in phase I clinical trial in advanced solid tumors, was evaluated in plasma collected in the first cycle of therapy within 21 days of the first administration of **ONC201** [12].

9. ONC201 STRUCTURE-ACTIVITY RELATIONSHIPS (SAR) STUDIES

ONC201 (also known as TIC10) was originally identified from the National Cancer Institute (NCI) chemical library for its ability to induce TRAIL (tumor necrosis factor-alpha-related apoptosis- inducing ligand) gene transcription in a human colon cancer cell line (HCT116).

The SAR of the ONC201 chemical series was investigated through an iterative process of chemical structure optimization and subsequent testing in cell viability assays [63, 64]. Importantly, the initial chemical structure for the compound was determined to be incorrect by Jacob *et al.* [65], spurring a series of synthetic efforts leading to the identification of novel chemical entities based on this newly discovered pharmacophore [66]. Madera Therapeutics created a series of novel highly potent analogs of ONC201 and defined a new chemical series collectively known as TR compounds [67-69]. In particular, **ONC201** aromatic rings (**A** and **B**) were extensively modified (Fig. **13**) by also applying a structure simplification approach.

ONC201 cytotoxicity was tested on different solid tumor cell lines and its activity did not exceed the order of the micromolar (Table **3**) [66]. The cytotoxic effect (with some exceptions) of **ONC201** and its analogs on the human colon (HCT216) and breast (MDA231) can-

cer cell lines was of the same order of magnitude (Table **4**) [63, 64, 67, 68, 70].

Table 3. ONC201 toxicity in some tumor cell lines.

Cell Line	ONC201 IC_{50} (μM)
Colo205	15.1 ± 3.3
KYSE140	58.1 ± 15.9
PC3	8.9 ± 3.2
MDA-MB-468	8.9 ± 1.6
H3122	8.7 ± 2.3
THP1	14.4 ± 4.5
RS4;11	31.4 ± 14.8
MV4;11	3.0 ± 1.3
Molm13	7.5 ± 1.9
Molm14	6.3 ± 2.2

As far as the compounds listed in Table **4** are concerned, when ring **A** has no substituent (R = H), **2** (ONC212) and **9** (ONC211) are obtained. They are the most potent derivatives and specifically have on the **B**-ring, a 4-CF_3 (IC_{50} = 0.03/0.05 μM), or a 3,4-dichloro (IC_{50} = 0.08/0.12 μM), respectively.

It is noteworthy, that the CF_3 position on the **B**-ring affects the potency of the corresponding compounds. In fact, when it is in *ortho*-position (**6**), the IC_{50} in the HCT116 cell line is 0.03 μM, in *meta*-position (**7**), the IC_{50} is 0.24 μM, and lately in *para*-position (**2**), the IC_{50} is 1.4 μM (in the MDA231 cell line the IC_{50} values are 0.05, 0.40 and 1.20 μM, respectively).

The presence of a 3-CH_3 on the **B**-ring associated with the condensation of the imidazole ring with cyclohexane lead to compound **5** which has a cytotoxic activity of 0.069 μM in the MDA231 cell line. The substitution of 4-CF_3 of **ONC212** (**2**) with 4-OCF_3 (**20**) decreased its potency. **20** has an IC_{50} of 0.37 and 0.82 μM in the two cell lines, respectively.

The subsequent substitutions also concern the ring **A**, providing several novel compounds (**4**, **14-19** and **24)** endowed with a higher potency of at least two orders of magnitude than **ONC201**. All of them are characterized by the presence of a halogen like chloride or bromide or isostere CF_3 in the para-position of the **B**-ring.

Another set of **ONC201** analogs were synthesized and tested to evaluate their antiproliferative activity in both human colon and breast cancer cell lines. In this series, the best result was obtained by substituting 2-CH_3 of **ONC201** on the benzyl **B,** with a 4-Cl (**I3**), a potency increase of two orders of magnitude was observed. Instead, the introduction in the **A** ring of **ONC201** a 2-F (**I15**), 3-Br (**I29**), or 3-CF_3 (**I9**) or a 3-CH_3 (**I34**) led to gain one more order of magnitude of cytotoxic effects. Keeping the 3-CH_3 in the phenyl **A** but substituting the 2-CH_3 in the phenyl **B** with a 2-CF_3 (**I33**) 2-Br (**I34**), compounds of very similar cytotoxic potency were obtained.

The substitution of 2-Cl with bromine (**I15**, **I14**, **I19**, **I26**, **I33**, **I37**, **I52**, **I55**) in ring **B** always determines a decrease of the potency, maybe to the higher size of the bromine atom. Definitely, with this skeleton, the only replacement that determines a remarkable gain in potency is that of **I3**.

Cytotoxicity of **ONC217**, **ONC223**, **ONC220**, **ONC218**, **ONC210**, **ONC213**, **ONC203**, **ONC22**, **ONC224**, **ONC226** was also evaluated in human lung fibroblast cell line (MRC-5) showing an IC_{50} ranging between <10 and <50 μM. On the other hand, **ONC2012**, **I4** (TR65), **TR42**, **I5** (TR66), and **4** (TR27) were tested on human triple-negative breast cancer cell line (SUM159) and were found to be cytotoxic with IC_{50} = 0.0014, 0.074, 0.14, 0.011 and 0.010 μM, respectively.

A new set of compounds obtained modifying the two benzyls present in **ONC201** (rings A and B) allowing the preparation of derivatives listed in Table **5**. Their cytotoxicity was evaluated on **HCT116**, **MDA 231**, and **MRC5** cell lines.

The tentative to reduce the size of the piperidine of **ONC201** led to compounds **I55-I58** of comparable potency to **ONC201** (Table **6**).

A structural simplification approach to study the structure-activity relationships of **ONC201** was then applied, obtaining a new series of compounds in which the dihydroimidazo-pyrimidinone core ring was substituted by a pyrimidine-2,4(1*H*,3*H*)-dione [69]. Their anticancer activity was measured by the CCK8 cell proliferation test (Table **7**).

The best results were obtained in the *N*-methyl and *N*-ethyl substituted derivatives, while opportune substituents in the **B** ring led to sub-micromolar cytotoxic compounds (**3**, **6**, and **11**) for both cell lines. No remarkable activity was observed with unsubstituted and isopropyl substituted derivatives.

Table 4. Anticancer activity measured by CCK8 assay.

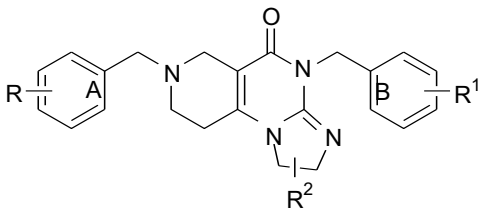

Compound[a]	R	R^1	R^2	HCT116[b] IC_{50} (μM)	MDA231[c] IC_{50} (μM)
ONC217	H	2-fluoro	H	<10	NF
ONC202		2-chloro		NF	NF
I5		2-bromo		5.96	6.81
6		2-trifluoromethyl		1.4	1.2
ONC201		2-methyl		2.8	3.0
I1		3-chloro		0.23	0.24
7		3-trifluoromethyl		0.24	0.40
I2		3-methyl		0.23	0.24
I3		4-chloro		0.06	0.07
2 (TR31-ONC212)[d]		4-trifluoromethyl		0.03	0.05
ONC223		4-methyl		<1	NF
20		4-trifluoromethoxy		0.37	0.82
ONC220		4-trifluoromethoxy		<0.5	NF
ONC206		2,4-difluoro		<0.5	NF
I41 (ONC219)		2,4-dichloro		1.73	2.01
ONC225		2-fluoro-4-trifluoromethyl		<1	NF
I43		2-trifluoromethyl-4-chloro		4.29	2.85
ONC218		2-methyl-4-fluoro		<0.5	NF
ONC 210		3,5-difluoro		<1	NF
9 (ONC 211)		3,4-dichloro		0.08	0.120
ONC213		3,4-difluoro		<1	NF
I42		3-trifluoromethyl- 4-chloro		0.73	1.07
ONC203		2-thienyl[e]		<10	NF
ONC222		3-isoxazolidinyl[e]		<10	NF
ONC224		methylen-(4-morpholinyl)[e]		<1	NF
ONC226		3-pyridinyl[e]		<1	NF
I16	2-bromo	2-fluoro		2.16	3.07

(Table 4) contd….

Compound[a]	R	R^1	R^2	HCT116[b] IC_{50} (μM)	MDA231[c] IC_{50} (μM)
I18	H	2-chloro	H	2.15	2.21
I19		2-bromo		2.22	3.67
I17		2- trifluoromethyl		2.02	2.14
10		2-methyl		>25	>25
I11	2-fluoro	2-fluoro		1.99	2.18
I13		2-chloro		1.77	1.94
I14		2-bromo		1.45	2.08
I12		2-trifluoromethyl		2.04	2.07
I15		2-methyl		0.68	0.73
I23	2-chloro	2-fluoro		2.00	2.14
I25		2-chloro		1.95	1.31
I26		2-bromo		1.50	2.08
I24		2-trifluoromethyl		2.09	1.99
I27		2-methylen		2.13	2.26
I21	2-methyl	2-fluoro		2.12	2.15
I45		2-chloro		ND	ND
I46		2-bromo		ND	ND
I22		2-trifluoromethyl		2.03	2.13
ONC229		4-trifluoromethyl		NF	NF
I47		2-methyl		ND	ND
I53	3-bromo	2-fluoro		0.70	0.73
I28		2-chloro		2.20	2.22
I48		2-bromo		ND	ND
I54		2-trifluoromethyl		21.41	24.78
11		2-methyl		0.72	0.74
I49	3-fluoro	2-fluoro		0.58	0.93
I51		2-chloro		0.70	0.73
16		4-chloro		0.028	0.070
I52		2-bromo		1.18	2.07
17		4-bromo		0.023	0.064
I50		2-trifluoromethyl		0.77	1.77
18		4-trifluoromethyl		0.022	0.078
I36	3-chloro	2-chloro		0.72	0.74
I37		2-bromo		2.31	2.33
27		4-trifluoromethyl		0.016	0.016
I30	3-methyl	2-fluoro		2.07	2.13
I32		2-chloro		0.77	0.74
I33		2-bromo		0.72	0.86

(Table 4) contd….

Compound[a]	R	R^1	R^2	HCT116[b] IC_{50} (μM)	MDA231[c] IC_{50} (μM)
I31	H	2-trifluoromethyl	H	1.25	1.65
I34		2-methyl		0.73	0.73
I35	3-chloro	2-trifluoromethyl		6.21	4.21
14 (TR65)[d]	3-nitrile	4-chloro		0.011	0.024
TR42[d]		4-bromo		ND	NF
15 (TR66)[d]		4-trifluoromethyl		0.007	0.024
3=21	3- trifluoromethoxy	4-trifluoromethyl		0.36	0.27
I9	3-trifluoromethyl	2-methyl		0.71	0.74
24		4-trifluoromethyl		0.087	0.22
13	3-methylidyne	4-bromo		0.28	0.28
4 (TR27)[d]		4-chloro		0.082	0.069
12		4-trifluoromethyl		0.22	0.22
8		4-trifluoromethoxy		1.8	0.88
22	4- methylidyne	4-chloro		1.8	3.4
23	4-fluoro	4-bromo		0.36	0.61
ONC228		4-trifluoromethyl		NF	NF
ONC227	4-trifluoromethyl	4-trifluoromethyl		NF	NF
ONC235	4-chloro	4-trifluoromethyl		NF	NF
ONC234	3,4-dichloro	4-trifluoromethyl		NF	NF
19	3-perdeuteriobenzyl[f]			0.089	ND
25	thiophene-2-ylmethyl[f]	4-chloro		1.7	0.71
26	thiophene-3-ylmethyl[f]	4-chloro		0.57	0.31
I10	4-(4-methylpiperazine)	2-methyl		2.09	2.19
I44	4-*t*-butyl	2-methyl	H	ND	ND
5	H	3-methyl	C_6H_{11}[g]	1.3	0.069

All the compounds are named as in the original documents [51, 64, 68, 70]; [a] NF: non found, ND: nondetermined; [b] HCT116: human colon cancer cell line; [c] MDA-231: human triple-negative breast cancer cell line; [d] [67]; [e] hetero ring substitutes phenyl B; [f] hetero ring substitutes the phenyl A; [g] C ring condensed with cyclohexyl.

Thus, new compounds were synthesized by adding to the **A** ring in the *N*-methyl and *N*-ethyl series a nitrile in *meta*-position. Compounds **26** and **28** became more potent than the corresponding benzyl derivatives **9** and **11** specifically towards the breast cancer cell line. A sub-micromolar activity was obtained also when, in the *N*-methyl series, a methyl substituted the methylidyne (**30**) reverting the preferential activity towards the hepatic cell line.

Chemical changes to the R^1 group produced compounds with a wide range of potency, many of which were much more potent than **ONC201**. Halogens within the benzyl R^1 group replacing the 2-methylbenzyl provide **ONC212** (4-trifluoromethylbenzyl group at R^1) more potent than **ONC201**, resulting in some cases in up to a 1000-fold reduction in GI50 on tumor cells without increased cytotoxicity toward normal cells. Other analogs with halide substituents in the R^1 group such as in **ONC206** (2,4-difluorobenzyl) and **ONC219** (2,4-dichlorobenzyl) were also potent in colorectal cancer (CRC) cell line and had a large *in vitro* therapeutic window. This suggests that replacing the R^1 group with halide benzyl groups increases potency. The widest separation between toxicity toward tumor cells *versus* normal cells was observed for compounds in which a group at the 2-position of the benzyl substituent was absent, such as **ONC212**, **ONC213** (3,4-difluorobenzyl) and **ONC211** (3,4-dichlorobenzyl). Variants at R^2 were also pre-

Table 5. Cytotoxic activity of a new set of synthesized ONC201 derivatives.

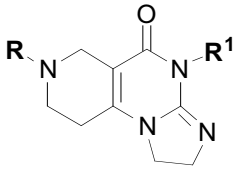

Compound[a]	R	R^1	HCT116[b] IC_{50} (μM)	MDA 231[c] IC_{50} (μM)	MRC5[d] IC_{50} (μM)
ONC207	H	2-methylbenzyl	<1	NF	<10
ONC221		4-methylbenzyl	<1	NF	<10
ONC208	methyl	2-methylbenzyl	NF	NF	NF
ONC204	methylbenzene	phenetyl	NF	NF	NF
ONC205		ethy(4-N-benzyl-piperazine)	NF	NF	NF
ONC209	ethylbenzene	2-methylbenzyl	NF	NF	NF
ONC215	*t*-butylethylcarbamate	2-methylbenzyl	NF	NF	NF
ONC216	aminopropyl	2-methylbenzyl	NF	NF	NF
ONC230	(4-fluorophenyl)--4-oxobutyl	4-trifluoromethylbenyl	NF	NF	NF
ONC231	methylen-3-pyridinyl	4-trifluoromethylbenzyl	NF	NF	NF
ONC232	methylen-4-methyl-2-tiazolyl	4-trifluoromethylbenziy	NF	NF	NF
ONC233	methylen-2-pyrazinyl	4-trifluoromethylbenzyl	NF	NF	NF
ONC236	methylen-3-thienyl	4-trifluoromethylbenzyl	NF	NF	NF
ONC237	phenylethanol	4-trifluoromethylbenzyl	NF	NF	NF

[a] Compounds are named as in the original documents [51, 64, 68-70]; [b] HCT116: human colon cancer cell line; [c] MDA-231: human triple-negative breast cancer cell line; [d] MRC-5: human lung fibroblast. **Abbreviations:** NF: not found in patents and/or published articles.

Table 6. Anticancer activity measured of I55-I58 by MTS cell proliferation test.

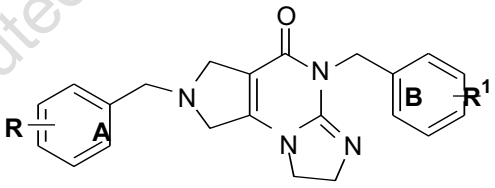

Compound[a]	R	R^1	HCT116[b] IC_{50} (μM)	MDA 231[c] IC_{50} (μM)
I55	H	2-bromo	2.14	2.19
I56		2,4-dichloro	2.05	2.05
I57		3-trifluoromehyl, 4-chloro	2.08	2.10
I58		2-methyl	not determined	not determined

[a] Compounds are named as in the original documents [51, 64, 68-70]; [b] HCT116: human colon cancer cell line; [c] MDA-231: human triple-negative breast cancer cell line.

Table 7. Anticancer activity measured by the MTS cell proliferation test.

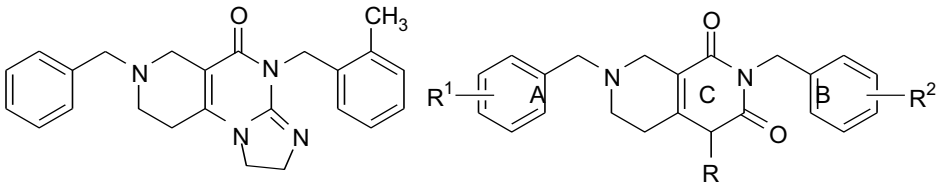

Compd[a]	R	R^1	R^2	HCT116[b] IC50 (μM)	MDA 231[c] IC50 (μM)	SUM159[d] IC50 (μM)
2	H	H	3-methyl	3.0	3.6	NF
5			4-chloro	2.7	10	NF
8			4-trifluomethyl	2.6	1.3	NF
1	methyl	H	H	ND	>100	NF
3			3-methyl	0.18	0.24	NF
6 (TR57)			4-chloro	0.26	0.29	0.014
9			4-trifluoromethyl	0.31	1.1	NF
13			3-trifluoromethyl	1.4	1.1	NF
15			3-chloro	3.0	2.1	NF
17			3-chloro	1.1	0.86	NF
23			[1,3]dioxole	2.5	2.6	NF
18		3-nitrile	4-trifluoromethyl	1.4	0.68	NF
19			2-methyl	1.5	1.1	NF
20			3-methyl	1.0	0.55	NF
21			4-chloro	1.4	0.63	NF
24			4-bromo	0.022	0.11	NF
25			4-chloro	0.74	0.19	NF
26			4-trifluoromethyl	0.50	0.085	NF
30		3-chloro	4-trifluoromethyl	0.098	0.29	NF
22			4-trifluoromethyl	0.1	0.29	NF
29		3-methyl	4-trifluoromethyl	ND	1.4	NF
11	ethyl	H	4-trifluoromethyl	0.75	0.23	NF
12			4-chloro	0.81	1.1	NF
14			3-trifluoromethyl	2.5	1.0	NF
16			3-chloro	1.8	3.3	NF
27		3-nitrile	4-trifluoromethyl	1.9	0.22	NF
28			4-chloro	0.21	0.022	NF
4	isopropyl	H	3-methyl	2.0	4.1	NF
7			4-chloro	6.6	14	NF
10			4-trifluoromethyl	7.1	4.0	NF
TR79	aminopropyl	3-nitrile	4-trifluoromethyl	NF	ND	0.057
TR80	aminobutyl	3-nitrile	4-trifluoromethyl	NF	ND	0.23
TR81	aminobutyl	3-nitrile	4-chloro	ND	ND	NF

[a] Compounds are named as in the original documents [51, 64, 68-70]; [b] HCT116: human colon cancer cell line; [c] MDA-231: human triple-negative breast cancer cell line; [d] SUM159: mesenchymal triple-negative breast cancer cell line.

pared, with **ONC207** (H) having no anticancer activity, while the potency was restored with manipulation of the R^1 group in **ONC221** (R^2-H; R^1-4- CF_3-benzyl group).

ONC212, a trifluoromethylbenzyl imipridone, and **ONC206**, a difluorobenzyl imipridone, were initially selected based on their GI50 in HCT116 cells compared to their effects on normal cells (an approximation of *in vitro* therapeutic window). The potencies of both analogs were evaluated in cancer cell lines across 10 tissue types and in an additional four normal cell lines. These experiments demonstrated that **ONC212** and **ONC206** have a nanomolar activity that is consistently more potent than **ONC201** across several tumor types. Both compounds also demonstrated the ability to inhibit colony growth of both colorectal and melanoma cancer cell lines. The results prompted further investigation of these analogs.

Interestingly, **ONC206** and **ONC201** both inhibited invasion and migration of tumor cells, while **ONC212** inhibited the only invasion. These observations on kinetics of response and invasion suggest that **ONC212** possesses distinct anticancer properties relative to other imipridones. **ONC212** was selected for *in vivo* evaluation considering the strong potency and differentiated kinetics of signaling.

10. STRUCTURAL STUDIES OF HUMAN (Hs)ClpP AND ITS BINDERS

New insights into the structural features and the proteolytic process mediated by the ClpP are gained from enough experimental data since the three-dimensional scaffold of the human isoform of this protein was determined in two diverse conditions. Firstly, the molecular assembly in the apo state was unraveled by X-ray crystallography in 2005 [71], and later on, in 2018, the first *holo* form in complex with the acyldepsipeptide **ADEP-28** (Table **1**) was solved [72], followed by the Y118A active mutant in complex with the oxadiazon-carboxyamide **D9** (Fig. **12**) [61]. In 2019, the crystals of the HsClpP/**ONC201** complex were obtained [49], and indeed a direct comparison between the *apo* and this latest *holo* form highlighted the most salient differences between the two states and furnished a perception on a plausible mechanism of action of HsClpP.

Both structures are organized as a heptameric channel-like pore (Fig. **14**), most likely representing the moiety where peptide products are expelled, but the **ONC201** binding to the active site region cause a slight modification of the entire molecular bundle, as proved by lower (1425 *vs.* 1505 $Å^2$) average contact surface area between each monomer, and a larger (17 *vs* 12 Å) distance between aspartate residues of each catalytic triad governing the proteolytic activity of HsClpP.

It must be pointed out that this evidence is not due to direct contact between **ONC201** and the aforementioned triad (Ser152, His178, and Asp227), but it is rather modulated by diverse interactions (*i.e.,* extensive hydrophobic contacts, π-π stacking and hydrogen bonds) gained with other residues defining a most likely allosteric, or at least secondary, binding site.

Additional clues revealing the chemical clichés, critical for the activity, are also gained by a comparison of the binding mode **ONC201** and **D9** as achieved by docking of these ligands to the HsClpP wild type. Both binders can largely fulfill the cavity formed by the α-helix and β-sheet motifs of two adjacent monomers of the heptameric bundle with similar chemical patterns: the three rings core of imipridone engages an extensive, water-mediated, network of hydrogen bonds with Gln107 and Tyr118, and further stabilizes the binding with additional hydrophobic contacts comprising its aromatic benzyl pendent and sidechains of Tyr138 and Leu104 (Fig. **15**).

A comparable pharmacophoric organization is also observed in the docking of **D9**, whose pose extremely resembles the **ONC201** binding mode, as assessed by a Tanimoto shape-based similarity coefficient equal to 0.848, with the oxazole overlapping the alicyclic moiety of the imipridone, and both the two aromatic terminals sharing the same hindrance suggest an analogous pharmacological profile for these binders (Fig. **16**).

11. OUTLINE OF CLINICAL TRIALS

The overall prognosis for children affected by DIPG remains poor. In the last decades, many reports have demonstrated that both radiotherapy and chemotherapy do not impact on the fatal course of the disease.

Early retrospective analysis showed that whole-brain irradiation has similar outcomes in comparison to the conservative approach of focal radiotherapy [73, 74]. Therefore, the standard of care of children with DIPG remains conventional focal radiotherapy with a treatment dose of 54-60 Gy in 1.8-Gy daily fractions over 6 weeks.

Following radiotherapy, most children obtain improvement in clinical symptoms and signs, although the benefit is transient with a marginal impact on progression-free survival. Radiotherapy appears to increase the overall survival of a few months with a mean progres-

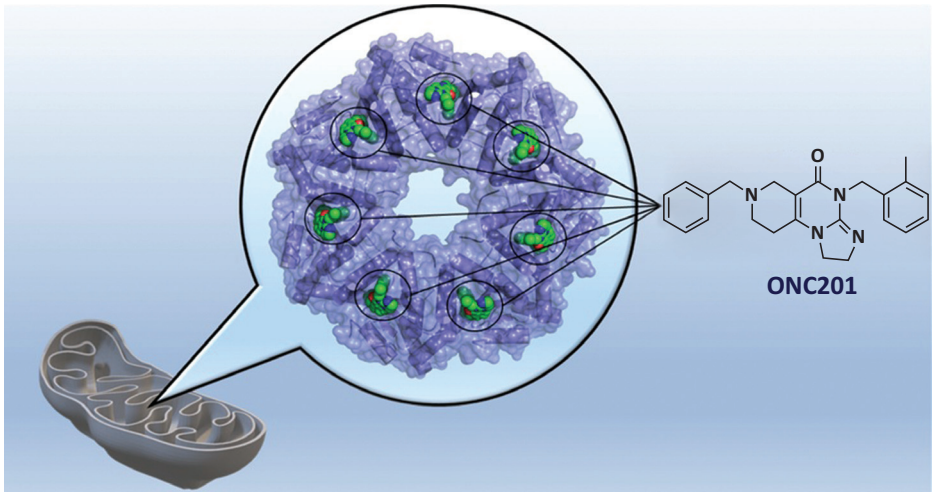

Fig. (14). Heptameric assembly of HsClpP. *(A higher resolution / colour version of this figure is available in the electronic copy of the article).*

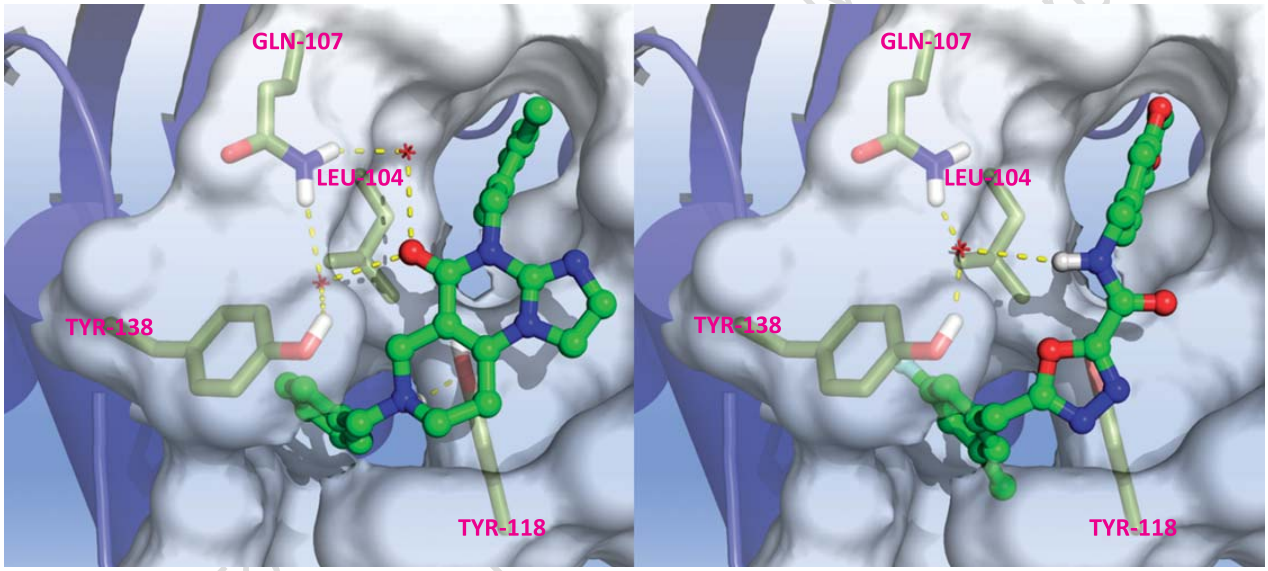

Fig. (15). Horizontal view of the docking relative to ONC201 (**left**) and D9 (**right**) into the HsClpP (pdb code: 6DL7). The estimated free energies of binding, measured according to the AutoDock scoring function, are 8.92 and -8,23 kcal/mol, respectively. Water molecules are represented as a single cross. *(A higher resolution / colour version of this figure is available in the electronic copy of the article).*

sion-free survival of only 5-6 months compared with 5 months for children with DIPG without focal irradiation [2].

In the 1980s and 1990s, attempts were made to enhance the potential efficacy of radiotherapy by using hyperfractionated schedules with twice-daily doses of 110-120 cGy. The Children's Cancer Group (CCG) and Pediatric Oncology Group (POG) tested hyperfractionated radiotherapy up to a total dose of 78 and 75.6 Gy, respectively. Both groups concluded that no clinical benefit was observed adopting hyperfractionated schedules over conventional radiotherapy at 54 Gy [75].

More recently, to improve the life quality of children with DIPG, hypofractionated delivery was evaluated. Zaghloul *et al.* randomized DIPG patients to receive 3 Gy daily for a total of 39 Gy over 3 weeks versus conventional 54 Gy in 30 fractions over 6 weeks. Limiting radiotherapy to 39 Gy over 3 weeks had a similar impact on overall survival but reduced toxicity with a shorter time that children spent in the hospital for the care delivery [76].

In recent years, a growing interest has emerged about the possibility of a re-irradiation of children with refractory or recurrent DIPG taking into account the lacking efficacy of other treatments. In a retrospective

review of the European Pediatric Oncology International Society (SIOP-E) 32 patients with DIPG received re-irradiation with a dose ranging from 18 to 30 Gy (fractions, 1.8-3 Gy) starting 3 or more months since the previous radiotherapy. Following re-irradiation, most patients had a clinical improvement [77]. Similar results were obtained on 16 patients with progressive DIPG who received further focal irradiation. Interestingly, the use of steroids was avoided and/or discontinued in many patients by the end of the re-irradiation [78].

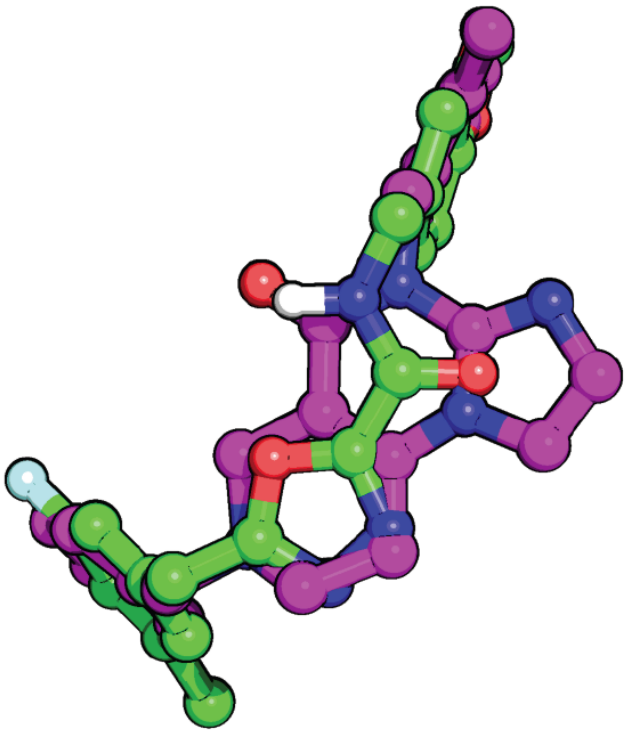

Fig. (16). Molecular superposition of the docking poses of **ONC201** (magenta carbons) and **D9** (green carbons). *(A higher resolution / colour version of this figure is available in the electronic copy of the article).*

The comparison with the historical cohorts of patients with DIPG receiving initial radiotherapy without re-irradiation suggests a potential neurological improvement and a benefit in overall survival following re-irradiation. However, several aspects of the DIPG re-irradiation option remain to be addressed, including the total radiation dose, fractioning, the interval from the previous radiotherapeutic treatment, risks of severe toxicities, and combination with antineoplastic agents.

Many small studies have attempted to use different antineoplastic agents as radiosensitizing with concomitant irradiation. Cisplatin concurrently administered with radiotherapy shown similar outcomes in children with DIPG when compared with radiation alone [79].

The Pediatric Brain Tumor Consortium (PBTC) phase II trial has used capecitabine during radiotherapy for children with newly diagnosed DIPG based on the evidence that glioma tumor cells express high levels of thymidine phosphorylase able to generate high concentrations of 5-fluorouracil in tumor tissue. Both capecitabine and 5-fluorouracil are radiation sensitizers and may enhance the therapeutic effect of radiotherapy. The use of capecitabine and concurrent radiotherapy also failed to provide an improvement in the overall survival of children with DIPG [80].

In adults with glioblastoma, temozolomide, an alkylating agent especially effective in O6-methylguanine DNA methyltransferase (MGMT) promoter methylated tumors, showed interesting activity when administered in combination with radiotherapy. Based on these data, a similar protocol was adopted in the challenging scenario of treating children with DIPG. However, no significant improvement in the outcome of children with DIPG receiving concomitant temozolomide and irradiation, followed by adjuvant temozolomide up to 10 cycles was obtained. The mean 1-year event-free survival and the mean 1-year overall survival were found to be 14% and 40%, respectively [81].

Similar conclusions emerged from other studies. In the trial performed by Chassot *et al.,* 21 patients received radiotherapy with concomitant and adjuvant temozolomide: the median progression-free survival and overall survival were 7.5 and 11.7 months, respectively [82]. Rizzo *et al.* treated 15 children with focal radiotherapy along with concurrent daily temozolomide followed by adjuvant temozolomide; the median progression-free survival was 7.15 months (range, 3.4–15.3 months), while the median overall survival was 15.6 months (range, 3.4-25.9 months) [83].

Similarly, attempts to improve the efficacy of focal radiotherapy in patients with DIPG adopting concurrent molecularly targeted agents such as imatinib and tipifarnib offered no clinical advantage over historical controls with radiation alone [84, 85].

The chemotherapy role as a standard treatment in the management of children with DIPG has yet to be established. Although some activity of several single and multiple agent chemotherapy regimens were reported, responses are generally short-lived and at present no regimen seems to be superior to others.

In 1977, the Children's Cancer Study Group evaluated, in a randomized prospective study involving 74 patients with DIPG, the efficacy of irradiation with and without adjuvant lomustine, vincristine, and predni-

sone. They concluded that the survival rate was irrespective of the adjuvant chemotherapy received for 1 year and was similar to treatment with irradiation alone; besides, the chemotherapeutic regimen was not able to delay the relapses [86].

The role of the pre-irradiation chemotherapy was also studied by the Children's Cancer Group (phase II trial CCG-994) adopting several possible combinations of alkylating and platin-based agents, and topoisomerase inhibitors. The 63 participants were randomized to receive two regimens of chemotherapeutic agents: carboplatin-etoposide-vincristine versus cisplatin-etoposide-cyclophosphamide-vincristine. Both groups of patients were then proceeded to hyperfractionated radiotherapy of 72 Gy. The results showed no significant difference in event-free survival and overall survival despite the relatively greater chemotherapy intensity of the second regimen with a similar 1-year event-free survival of 17% (95% CI 7.2–26.8%) [87].

The poor outcome of children with DIPG led to trials with other different drugs such as carboplatin, nitrosurea compounds, cyclophosphamide, ifosphamide, oral etoposide, and tamoxifene [88, 89]. Objective responses were rare and limited with no consistent effect on survival or outcome.

Due to this uniformly poor outcome for patients with newly diagnosed DIPG, a high dose chemotherapy regimen has been investigated by some authors with anecdotal reports or small series. In a Societè Francaise d'Oncologie Pediatrique (SFOP) pilot study, 24 consecutive children with a newly diagnosed DIPG received systematically high-dose chemotherapy with busulfan-thiotepa after irradiation. The busulfan-thiotepa combination was based on pharmacological data showing that both drugs can cross the blood-brain barrier (BBB). All enrolled patients died, 3 of toxic complications, and 21 of disease progression. The median survival time for non-transplanted patients (most of them because of early disease progression) was 8±1.5 months versus 10±2.6 months for the arm of transplanted patients.

In recent years, other different approaches were attempted in children with refractory DIPG such as intra-arterial or intra-nasal chemotherapy, and convection-enhanced drug delivery (CED). All these approaches were developed to bypass the BBB as DIPGs have a relatively intact blood-brain barrier. CED is based on a surgical technique utilizing a catheter to deliver the drug directly into the tumor through a pump. By this system, macromolecules, such as monoclonal antibodies (*i.e.* 8H9), irinotecan liposome, and nanoparticle formulation of panobinostat MTX110 have been delivered to the tumor [90-92]. Recent trials have evaluated the addition of various targeted agents such as tyrosine kinase inhibitors (*i.e.* dasatinib, ponatinib, imatinib, pazopanib, sunitinib), PI3K/mTOR pathway inhibitors (*i.e.* LY3023414, everolimus) or antiangiogenetic agents (*i.e.* thalidomide) but all have failed to significantly prolong the survival of children with DIPG [93, 94]. Novel therapeutic approaches including multimodal therapy consisting of Newcastle disease virus, hyperthermia, and autologous dendritic cell vaccines [95], inhibitors of ALK2 (K02288, LDN-213844, and LDN-214117) [96], and selective LSD1 inhibition have been proposed as part of an individualized treatment approach for DIPG patients [97]. All clinical trials regarding DIPG are reported in Table **8**.

CONCLUSION

DIPG remains a tumor with a dismal prognosis. Despite advances in neurosurgical techniques and radiotherapy delivery, little improvement in prognosis has been achieved with limited influence on the natural course of the disease. Several clinical studies with novel agents have been performed or are underway to find a more active medical treatment.

At present, **ONC 201** represents the only drug for the treatment of DIPG on which there are many hopes. The great interest is derived from signs of efficacy obtained in adults and children affected by high-grade gliomas. Phase II clinical studies at the Massachusetts General Hospital Cancer Center on 17 patients with recurrent bevacizumab-naive glioblastoma treated with the oral capsule of **ONC201**, once every 3 weeks (21-day cycle), showed promising results. The progression-free survival at 6 months was 11.8%, and two patients remained on therapy for greater than 11 months. The median overall survival (OS) of patients enrolled in the trial was 41.6 weeks, with the OS at 6 months being 71% [98]. In the USA, the Network Radiation Oncology/Children's Oncology Group (NRG/COG) cooperative group phase II trial is undergoing to test the efficacy of the **ONC201** in newly diagnosed DIPG, as well as newly diagnosed non-DIPG H3 K27M glioma. **ONC201** will be administered with irradiation and followed by maintenance **ONC201**. In Europe, the new BIOMEDE trial will include **ONC201** for children diagnosed with H3 K27M-mutant and/or H3K27me3-negative DIPG. Nevertheless, these trails will support further clinical development of the **ONC201** drug in children with DIPG but more effective drugs are required for this uniformly lethal tumor.

Table 8. Published and ongoing clinical trials in DIPG.

NCT NUMBER	TREATMENTS	PART.[a]	PHASE	STARTING DATE	RECRUIT-MENT STATUS
NCT04250064	Bevacizumab/Ultra-low-dose radiation therapy	40	II	2020	Recruiting
NCT01688401	Melphalan hidrocloride	3	I	2013	Active, not recruiting
NCT01952769	MDV9300	50	II	2014	Enrolling by invitation
NCT02274987	Standard radiation therapy	38	NA[b]	2014	Completed
NCT02233049	Erlotinib/Everolimus/Dasatinib	250	II	2014	Active, not recruiting
NCT02644460	Abemaciclib	60	I	2015	Recruiting
NCT02840123	Autologous dendritic cells	10	I	2016	Active, not recruiting
NCT03355794	Ribociclib/Everolimus	24	I	2017	Active, not recruiting
NCT03086616	Nanoliposomal Irinotecan	19	I	2017	Terminate[d]
NCT01777633	Palliative re-irradiation	15	II	2013	Active, not recruiting
NCT03841435	Hypofractionated radiation therapy	6	NA[b]	2018	Recruiting
NCT01644773	Crizotinib/Dasatinib	36	I	2012	Not yet recruiting
NCT02960230	K27M peptide/ Nivolumab	49	II	2016	Unknown
NCT02992015	Gemcitabine	10	I	2016	Completed
NCT03566199	Panobinostat Nanoparticle Formulation MTX110	24	II	2018	Completed
NCT02758366	Doxorubicin	20	II	2016	Unknown
NCT01182350	Bevacizumab/ Erlotinib/ Temozolomide/ radiation therapy	53	II	2011	Completed
NCT02420613	Laboratory Biomarker / Radiation Therapy/ Temsirolimus/ Vorinostat	6	I	2015	Recruiting
NCT00996723	Vandetanib and Dasatinib	25	I	2009	Recruiting
NCT03126266	Re-irradiation	25	NA[b]	2017	Recruiting
NCT04049669	Indoximod/ Partial Radiation/ Full-dose Radiation/ Temozolomide/ Cyclophosphamide/ Etoposide/ Lomustine	140	II	2019	Recruiting
NCT02359565	Pembrolizumab	110	I	2015	Recruiting
NCT04185038	SCRI-CARB7H3(s); B7H3-specific chimeric antigen receptor (CAR) T cell	70	I	2019	Recruiting
NCT03605550	PTC596/ radiation therapy	54	I	2018	Active, not recruiting
NCT02717455	LBH589	40	I	2016	Recruiting
NCT03178032	DNX-2401	12	I	2017	Completed
NCT01922076	Radiation Therapy	77	I	2013	Active, not recruiting
NCT03620032	Nimotuzumab/Vinorelbine/ radiation therapy	54	II	2018	Recruiting

(Table 8) contd….

NCT NUMBER	TREATMENTS	PART.[a]	PHASE	STARTING DATE	RECRUIT-MENT STATUS
NCT03893487	Fimepinostat	30	I	2019	Recruiting
NCT02750891	DSP-7888	18	I/II	2016	Completed
NCT00036569	Pegylated interferon alfa	32	II	2002	Completed
NCT03696355	Drug: GDC-0084/radiation therapy	41	I	2018	Active, not recruiting
NCT01517776	Cilengitide/Temozolomide	28	II	2012	Terminated
NCT00600054	Nimotuzumab	44	II	2008	Completed
NCT01058850	Rindopepimut	3	I	2010	Terminated
NCT04099797	(C7R)-GD2.CART cells/Cyclophosphamide/Fludarabine	34	I	2019	Recruiting
NCT04264143	Infusate with MTX110 and Gadolinium	9	I	2020	Recruiting
NCT00879437	Valproic acid/Bevacizumab/radiation therapy	38	II	2009	Active, not recruiting
NCT00028795	Temozolomide/radiation therapy	170	II	2003	Completed
NCT01445288	Radiation therapy	76	NR[c]	2011	Completed
NCT03598244	Savolitinib	36	I	2018	Recruiting
NCT02444546	Sargramostim/Wild-type Reovirus	6	II	2015	Active, not re-cruiting

[a]Partecipants; [b]NA=Not applicable; [c]NR=Not reported. [d]Treatment ineffective; Extreme toxicity;

An extensive **ONC201** structure-activity relationship was performed, and new compounds were developed. Several of these compounds showed cytotoxic activity at a different extent on the colon cancer cell lines, and a few more were deeply investigated. The identification of ClpP as a direct biological target of **ONC201** provides fertile ground to scientists' work in searching new molecules that can be used for the treatment of DIPG and may lead to performing a neonatal or even better prenatal screening for the early diagnosis of this disease.

As children and adults with DIPG, and general gliomas, are waiting for a drug to treat their disease, such pediatric cancer should be considered a hot topic, and direct great scientific efforts should be implemented on priority.

LIST OF ABBREVIATIONS

ADEPs = Acyldepsipeptides

BBB = Blood-brain Barrier

CAR-T = Chimeric Antigen Receptor

CBP = Creb-binding Protein

CCG = Children's Cancer Group

CED = Convectionenhanced Drug Delivery

ClPP = Caseynolitic Protease P

DCR = Decoy Receptors

DIPG = Diffuse Intrinsic Pontine Glioma

DISC = Death-Inducing Signaling Complex

DR = Dopamine Receptors

DR = Death Receptors

ERα = Estrogen Receptor α

FADD = Fas-Associated Protein With Death Domain

FKH = Forkhead

FOX = Forkhead Box Proteins

GPCRs = G-protein Coupled Receptors

HCT116 = Human Colorectal Carcinoma 116

HsClpP = Humans Clpp

HsClpX = Humans Clpx

ISR = Integrated Stress Response

MGMT = O6-Methylguanine Dna Methyltransferase

MTDNA = Mitochondrial Dna

MTS = Mitochondrial Targeting Sequence

NCI = National Cancer Institute

NES = Nuclear Export Sequence

NLS = Nuclear Localization Sequences

NRG/COG = Network Radiation Oncology/ Children's Oncology Group

OPG = Osteoprotegerin

OS = Overall Survival

PBTC = Pediatric Brain Tumor Consortium

PI3K = Phosphoinositol-3-Kinase

POG = Pediatric Oncology Group

SAR = Structure-Activity Relationship

SFOP = Societè Francaise d'oncologie Pediatrique

SIOP-E = European Pediatric Oncology International Society

TAD = Transactivation Domain

TBID = Truncated Bid

TRAIL = Tumor Necrosis Factor-Related Apoptosis-Inducing Ligand

UPR^{mt} = Mitochondrial Unfolded Protein Response

ZBD = Zinc-Binding Domain

DEDICATION

This review was inspired by the six years old little angel Arianna, and dedicated to all parents who hope in the scientific research to save their little warriors.

CONSENT FOR PUBLICATION

Not applicable.

FUNDING

This paper has received financial support by the Itel Telecomunicazioni srl Ruvo di Puglia (BA)-Italy) for providing a grant to A.C. and Associazione Mia Neri Foundation Onlus www.mianerifoundation.it, Rome-Italy and Associazione Progetto G.A.I.A.

CONFLICT OF INTEREST

Dr. Antonio Scilimati is serving as an editorial board member for the journal Current Medicinal Chemistry.

ACKNOWLEDGEMENTS

We thank Itel Telecomunicazioni srl Ruvo di Puglia (BA)-Italy) for providing a grant to A.C. and Associazione Mia Neri Foundation Onlus www. mianerifoundation.it, Rome-Italy and Associazione Progetto G.A.I.A. for supporting our research in pediatric oncology.

REFERENCES

[1] Harris, W. Case of pontine glioma, with special reference to the paths of gustatory sensation. *Proc. R. Soc. Med.,* **1926**, *19*(Neurol Sect), 1-5. http://dx.doi.org/10.1177/003591572601900901 PMID: 19985059

[2] Freeman, C.R.; Farmer, J.P. Pediatric brain stem gliomas: a review. *Int. J. Radiat. Oncol. Biol. Phys.,* **1998**, *40*(2), 265-271. http://dx.doi.org/10.1016/S0360-3016(97)00572-5 PMID: 9457808

[3] Cooney, T.; Lane, A.; Bartels, U.; Bouffet, E.; Goldman, S.; Leary, S.E.S.; Foreman, N.K.; Packer, R.J.; Broniscer, A.; Minturn, J.E.; Shih, C.S.; Chintagumpala, M.; Hassall, T.; Gottardo, N.G.; Dholaria, H.; Hoffman, L.; Chaney, B.; Baugh, J.; Doughman, R.; Leach, J.L.; Jones, B.V.; Fouladi, M.; Warren, K.E.; Monje, M. Contemporary survival endpoints: an International Diffuse Intrinsic Pontine Glioma Registry study. *Neuro-oncol.,* **2017**, *19*(9), 1279-1280. http://dx.doi.org/10.1093/neuonc/nox107 PMID: 28821206

[4] Hargrave, D.; Bartels, U.; Bouffet, E. Diffuse brainstem glioma in children: critical review of clinical trials. *Lancet Oncol.,* **2006**, *7*(3), 241-248. http://dx.doi.org/10.1016/S1470-2045(06)70615-5 PMID: 16510333

[5] Gupta, N.; Goumnerova, L.C.; Manley, P.; Chi, S.N.; Neuberg, D.; Puligandla, M.; Fangusaro, J.; Goldman, S.; Tomita, T.; Alden, T.; DiPatri, A.; Rubin, J.B.; Gauvain, K.; Limbrick, D.; Leonard, J.; Geyer, J.R.; Leary, S.; Browd, S.; Wang, Z.; Sood, S.; Bendel, A.; Nagib, M.; Gardner, S.; Karajannis, M.A.; Harter, D.; Ayyanar, K.; Gump, W.; Bowers, D.C.; Weprin, B.; MacDonald, T.J.; Aguilera, D.; Brahma, B.; Robison, N.J.; Kiehna, E.; Krieger, M.; Sandler, E.; Aldana, P.; Khatib, Z.; Ragheb, J.; Bhatia, S.; Mueller, S.; Banerjee, A.; Bredlau, A-L.; Gururangan, S.; Fuchs, H.; Cohen, K.J.; Jallo, G.; Dorris, K.; Handler, M.; Comito, M.; Dias, M.; Nazemi, K.; Baird, L.; Murray, J.; Lindeman, N.; Hornick, J.L.; Malkin, H.; Sinai, C.; Greenspan, L.; Wright, K.D.; Prados, M.; Bandopadhayay, P.; Ligon, K.L.; Kieran, M.W. Prospective feasibility and safety assessment of surgical biopsy for patients with newly diagnosed diffuse intrinsic pontine glioma. *Neuro-oncol.,* **2018**, *20*(11), 1547-1555. http://dx.doi.org/10.1093/neuonc/noy070 PMID: 29741745

[6] Schwartzentruber, J.; Korshunov, A.; Liu, X-Y.; Jones, D.T.W.; Pfaff, E.; Jacob, K.; Sturm, D.; Fontebasso, A.M.; Quang, D.A.; Tönjes, M.; Hovestadt, V.; Albrecht, S.; Kool, M.; Nantel, A.; Konermann, C.; Lindroth, A.; Jäger, N.; Rausch, T.; Ryzhova, M.; Korbel, J-O.; Hielscher, T.; Hauser, P.; Garami, M.; Klekner, A.; Bognar, L.; Ebinger, M.; Schuhmann, M.U.; Scheurlen, W.; Pekrun, A.; Frühwald, M.C.; Roggendorf, W.; Kramm, C.; Dürken, M.; Atkinson, J.; Lepage, P.; Montpetit, A.; Zakrzewska, M.; Zakrzewski, K.; Liberski, P.P.; Dong, Z.; Siegel, P.; Kulozik, A.E.; Zapatka, M.; Guha, A.; Malkin, D.; Felsberg, J.; Reifenberger, G.; von Deimling, A.; Ichimura, K.; Collins, V.P.; Witt, H.; Milde, T.; Witt, O.; Zhang, C.; Castelo-Branco, P.; Lichter, P.; Faury, D.; Tabori, U.; Plass, C.; Majewski, J.; Pfister, S.M.; Jabado, N. Driver mutations in histone $H_{3.3}$ and chromatin remodelling genes in paediatric glioblastoma. *Nature,* **2012**, *482*(7384), 226-231. http://dx.doi.org/10.1038/nature10833 PMID: 22286061

[7] Louis, D.N.; Perry, A.; Reifenberger, G.; von Deimling, A.; Figarella-Branger, D.; Cavenee, W.K.; Ohgaki, H.; Wiestler, O.D.; Kleihues, P.; Ellison, D.W. The 2016 World

Health Organization classification of tumors of the central nervous system: a summary. *Acta Neuropathol.,* **2016**, *131*(6), 803-820. http://dx.doi.org/10.1007/s00401-016-1545-1 PMID: 27157931

[8] Robison, N.J.; Kieran, M.W. Diffuse intrinsic pontine glioma: a reassessment. *J. Neurooncol.,* **2014**, *119*(1), 7-15. http://dx.doi.org/10.1007/s11060-014-1448-8 PMID: 24792486

[9] Li, J.; Zhu, S.; Kozono, D.; Ng, K.; Futalan, D.; Shen, Y.; Akers, J.C.; Steed, T.; Kushwaha, D.; Schlabach, M.; Carter, B.S.; Kwon, C-H.; Furnari, F.; Cavenee, W.; Elledge, S.; Chen, C.C. Genome-wide shRNA screen revealed integrated mitogenic signaling between dopamine receptor D_2 (DRD_2) and epidermal growth factor receptor (EGFR) in glioblastoma. *Oncotarget,* **2014**, *5*(4), 882-893. http://dx.doi.org/10.18632/oncotarget.1801 PMID: 24658464

[10] Langmoen, I.A.; Lundar, T.; Storm-Mathisen, I.; Lie, S.O.; Hovind, K.H. Management of pediatric pontine gliomas. *Childs Nerv. Syst.,* **1991**, *7*(1), 13-15. http://dx.doi.org/10.1007/BF00263825 PMID: 2054800

[11] *Pubmed source and DIPG used as a keyword*, 1989-2020. Available at: https://pubmed.ncbi.nlm.nih.gov/? term = diffuse+intrinsic+pontine+glioma&filter=dates.1989-2020& sort=date

[12] Allen, J.E.; Krigsfeld, G.; Mayes, P.A.; Patel, L.; Dicker, D.T.; Patel, A.S.; Dolloff, N.G.; Messaris, E.; Scata, K.A.; Wang, W.; Zhou, J.-Y.; Wu, G.S.; El-Deiry, W.S. Dual inactivation of Akt and ERK by TIC10 signals Foxo3a nuclear translocation, TRAIL gene induction, and potent antitumor effects. *Sci. Transl. Med.,* **2013**, *5*(171), 171ra17. http://dx.doi.org/10.1126/scitranslmed.3004828 PMID: 23390247

[13] Caragher, S.P.; Hall, R.R.; Ahsan, R.; Ahmed, A.U. Monoamines in glioblastoma: complex biology with therapeutic potential. *Neuro-oncol.,* **2018**, *20*(8), 1014-1025. http://dx.doi.org/10.1093/neuonc/nox210 PMID: 29126252

[14] Madhukar, N.S.; Elemento, O.; Benes, C.H.; Garnett, M.J.; Stein, M.; Bertino, J.R.; Kaufman, H.L.; Arrillaga-Romany, I.; Batchelor, T.T.; Schalop, L.; Oster, W.; Stogniew, M.; Andreeff, M.; El-Deiry, W.S.; Allen, J.E. Proceedings of the 107th Annual Meeting of the American Association for Cancer Research (AACR), New Orleans, LA, Philadelphia (PA)April 16-20, **2016**.

[15] Allen, J.E.; Krigsfeld, G.; Patel, L.; Mayes, P.A.; Dicker, D.T.; Wu, G.S.; El-Deiry, W.S. Identification of TRAIL-inducing compounds highlights small molecule ONC201/TIC10 as a unique anti-cancer agent that activates the TRAIL pathway. *Mol. Cancer,* **2015**, *14*(99), 99. http://dx.doi.org/10.1186/s12943-015-0346-9 PMID: 25927855

[16] Refaat, A.; Abd-Rabou, A.; Reda, A. TRAIL combinations: the new 'trail' for cancer therapy (Review). *Oncol. Lett.,* **2014**, *7*(5), 1327-1332. http://dx.doi.org/10.3892/ol.2014.1922 PMID: 24765133

[17] Ukrainskaya, V.M.; Stepanov, A.V.; Glagoleva, I.S.; Knorre, V.D.; Belogurov, A.A. Death receptors: new opportunities in cancer therapy. *Acta Naturae,* **2017**, *9*(3), 55-63. PMID: 29104776

[18] Dai, X.; Zhang, J.; Arfuso, F.; Chinnathambi, A.; Zayed, M-E.; Alharbi, S.A.; Kumar, A.P.; Ahn, K.S.; Sethi, G. Targeting TNF-related apoptosis-inducing ligand (TRAIL) receptor by natural products as a potential therapeutic approach for cancer therapy. *Exp. Biol. Med. (Maywood),* **2015**, *240*(6), 760-773. http://dx.doi.org/10.1177/1535370215579167 PMID: 25854879

[19] Allen, J.E.; Kline, C.L.B.; Prabhu, V.V.; Wagner, J.; Ishizawa, J.; Madhukar, N.; Lev, A.; Baumeister, M.; Zhou, L.; Lulla, A.; Stogniew, M.; Schalop, L.; Benes, C.; Kaufman, H.L.; Pottorf, R.S.; Nallaganchu, B.R.; Olson, G.L.; Al-Mulla, F.; Duvic, M.; Wu, G.S.; Dicker, D.T.; Talekar, M.K.; Lim, B.; Elemento, O.; Oster, W.; Bertino, J.; Flaherty, K.; Wang, M.L.; Borthakur, G.; Andreeff, M.; Stein, M.; El-Deiry, W.S. Discovery and clinical introduction of first-in-class imipridone ONC201. *Oncotarget,* **2016**, *7*(45), 74380-74392. http://dx.doi.org/10.18632/oncotarget.11814 PMID: 27602582

[20] Kline, C.L.B.; Van den Heuvel, A.P.; Allen, J.E.; Prabhu, V.V.; Dicker, D.T.; El-Deiry, W.S. ONC201 kills solid tumor cells by triggering an integrated stress response dependent on ATF4 activation by specific eIF2α kinases. *Sci. Signal.,* **2016**, *9*(415), ra18. http://dx.doi.org/10.1126/scisignal.aac4374 PMID: 26884600

[21] Allen, J.E.; Crowder, R.N.; El-Deiry, W.S. First-in-class small molecule ONC201 induces DR5 and cell death in tumor but not normal cells to provide a wide therapeutic index as an anti-cancer agent. *PLoS One,* **2015**, *10*(11), e0143082. http://dx.doi.org/10.1371/journal.pone.0143082 PMID: 26580220

[22] Greer, Y.E.; Porat-Shliom, N.; Nagashima, K.; Stuelten, C.; Crooks, D.; Koparde, V.N.; Gilbert, S.F.; Islam, C.; Ubaldini, A.; Ji, Y.; Gattinoni, L.; Soheilian, F.; Wang, X.; Hafner, M.; Shetty, J.; Tran, B.; Jailwala, P.; Cam, M.; Lang, M.; Voeller, D.; Reinhold, W.C.; Rajapakse, V.; Pommier, Y.; Weigert, R.; Linehan, W.M.; Lipkowitz, S. ONC201 kills breast cancer cells *in vitro* by targeting mitochondria. *Oncotarget,* **2018**, *9*(26), 18454-18479. http://dx.doi.org/10.18632/oncotarget.24862 PMID: 29719618

[23] Ralff, M.D.; Kline, C.L.B.; Küçükkase, O.C.; Wagner, J.; Lim, B.; Dicker, D.T.; Prabhu, V.V.; Oster, W.; El-Deiry, W.S. ONC201 demonstrates anti-tumor effects in both triple negative and non-triple negative breast cancers through TRAIL-dependent and TRAIL-independent mechanisms. *Mol. Cancer Ther.,* **2017**, *16*(7), 1290-1298. http://dx.doi.org/10.1158/1535-7163.MCT-17-0121 PMID: 28424227

[24] Ishizawa, J.; Kojima, K.; Chachad, D.; Ruvolo, P.; Ruvolo, V.; Jacamo, R.O.; Borthakur, G.; Mu, H.; Zeng, Z.; Tabe, Y.; Allen, J.E.; Wang, Z.; Ma, W.; Lee, H.C.; Orlowski, R.; Sarbassov, D.; Lorenzi, P.L.; Huang, X.; Neelapu, S.S.; McDonnell, T.; Miranda, R.N.; Wang, M.; Kantarjian, H.; Konopleva, M.; Davis, R.E.; Andreeff, M. ATF4 induction through an atypical integrated stress response to ONC201 triggers p53-independent apoptosis in hematological malignancies. *Sci. Signal.,* **2016**, *9*(415), ra17. http://dx.doi.org/10.1126/scisignal.aac4380 PMID: 26884599

[25] Yuan, X.; Kho, D.; Xu, J.; Gajan, A.; Wu, K.; Wu, G.S. ONC201 activates ER stress to inhibit the growth of triple-negative breast cancer cells. *Oncotarget,* **2017**, *8*(13), 21626-21638. http://dx.doi.org/10.18632/oncotarget.15451 PMID: 28423492

[26] Cao, Z.; Liao, Q.; Su, M.; Huang, K.; Jin, J.; Cao, D. AKT and ERK dual inhibitors: The way forward? *Cancer Lett.,* **2019**, *459*, 30-40. http://dx.doi.org/10.1016/j.canlet.2019.05.025 PMID: 31128213

[27] Liu, Y.; Ao, X.; Ding, W.; Ponnusamy, M.; Wu, W.; Hao, X.; Yu, W.; Wang, Y.; Li, P.; Wang, J. Critical role of FOXO3a in carcinogenesis. *Mol. Cancer,* **2018**, *17*(1), 104. http://dx.doi.org/10.1186/s12943-018-0856-3 PMID: 30045773

[28] Hannenhalli, S.; Kaestner, K.H. The evolution of Fox genes and their role in development and disease. *Nat. Rev. Genet.,* **2009**, *10*(4), 233-240. http://dx.doi.org/10.1038/nrg2523 PMID: 19274050

[29] Nho, R.S.; Hergert, P. FoxO3a and disease progression. *World J. Biol. Chem.,* **2014**, *5*(3), 346-354. http://dx.doi.org/10.4331/wjbc.v5.i3.346 PMID: 25225602

[30] Klotz, L-O.; Sánchez-Ramos, C.; Prieto-Arroyo, I.; Urbánek, P.; Steinbrenner, H.; Monsalve, M. Redox regulation of FoxO transcription factors. *Redox Biol.,* **2015**, *6*, 51-72. http://dx.doi.org/10.1016/j.redox.2015.06.019 PMID: 26184557

[31] Wang, X.; Hu, S.; Liu, L. Phosphorylation and acetylation modifications of FOXO3a: Independently or synergistically? *Oncol. Lett.,* **2017**, *13*(5), 2867-2872. http://dx.doi.org/10.3892/ol.2017.5851 PMID: 28521392

[32] Yang, W.; Dolloff, N.G.; El-Deiry, W.S. ERK and MDM2 prey on FOXO3a. *Nat. Cell Biol.,* **2008**, *10*(2), 125-126. http://dx.doi.org/10.1038/ncb0208-125 PMID: 18246039

[33] Yang, J-Y.; Hung, M-C. A new fork for clinical application: targeting forkhead transcription factors in cancer. *Clin. Cancer Res.,* **2009**, *15*(3), 752-757. http://dx.doi.org/10.1158/1078-0432.CCR-08-0124 PMID: 19188143

[34] Beretta, G.L.; Corno, C.; Zaffaroni, N.; Perego, P. Role of FoxO proteins in cellular response to antitumor agents. *Cancers (Basel),* **2019**, *11*(1), 90. http://dx.doi.org/10.3390/cancers11010090 PMID: 30646603

[35] Madhukar, N.S.; Khade, P.; Huang, L.; Gayvert, K.; Galletti, G.; Stogniew, M.; Allen, J.E.; Giannakakou, P.; Elemento, O. A new big-data paradigm for target identification and drug discovery. *bioRxiv,* **2017**, 134973. [Preprint paper]. https://doi.org/10.1101/134973

[36] Kline, C.L.B.; Ralff, M.D.; Lulla, A.R.; Wagner, J.M.; Abbosh, P.H.; Dicker, D.T.; Allen, J.E.; El-Deiry, W.S. Role of dopamine receptors in the anticancer activity of ONC201. *Neoplasia,* **2018**, *20*(1), 80-91. http://dx.doi.org/10.1016/j.neo.2017.10.002 PMID: 29216597

[37] Prabhu, V.V.; Madhukar, N.S.; Gilvary, C.; Kline, C.L.B.; Oster, S.; El-Deiry, W.S.; Elemento, O.; Doherty, F.; VanEngelenburg, A.; Durrant, J.; Tarapore, R.S.; Deacon, S.; Charter, N.; Jung, J.; Park, D.M.; Gilbert, M.R.; Rusert, J.; Wechsler-Reya, R.; Arrillaga-Romany, I.; Batchelor, T.T.; Wen, P.Y.; Oster, W.; Allen, J.E. Dopamine receptor D5 is a modulator of tumor response to dopamine receptor D2 antagonism. *Clin. Cancer Res.,* **2019**, *25*(7), 2305-2313. http://dx.doi.org/10.1158/1078-0432.CCR-18-2572 PMID: 30559168

[38] Birtwistle, J.; Baldwin, D. Role of dopamine in schizophrenia and Parkinson's disease. *Br. J. Nurs.,* **1998**, *7*(14), 832-834, 836, 838-841. http://dx.doi.org/10.12968/bjon.1998.7.14.5636 PMID: 9849144

[39] Cheng, H.W.; Liang, Y.H.; Kuo, Y.L.; Chuu, C.P.; Lin, C.Y.; Lee, M.H.; Wu, A.T.; Yeh, C.T.; Chen, E.I.; Whang-Peng, J.; Su, C.-L.; Huang, C-Y.F. Identification of thioridazine, an antipsychotic drug, as an antiglioblastoma and anticancer stem cell agent using public gene expression data. *Cell Death Dis.,* **2015**, *6*(5), e1753. http://dx.doi.org/10.1038/cddis.2015.77 PMID: 25950483

[40] Chi, A.S.; Stafford, J.M.; Sen, N.; Possemato, R.; Placantonakis, D.; Hidalgo, E.T.; Harter, D.; Wisoff, J.; Golfinos, J.; Arrillaga-Romany, I.; Batchelor, T.; Wen, P.; Wakimoto, H.; Cahill, D.; Allen, J.E.; Oster, W.; Snuderl, M. Exth-42. H_3K27M mutant gliomas are selectively killed by ONC201, a small molecule inhibitor of dopamine receptor D2. *Neuro-Oncology,* **2017**, *19*(suppl_6), vi81. http://dx.doi.org/10.1093/neuonc/nox168.334

[41] Stein, M.N.; Bertino, J.R.; Kaufman, H.L.; Mayer, T.; Moss, R.; Silk, A.; Chan, N.; Malhotra, J.; Rodriguez, L.; Aisner, J.; Aiken, R.D.; Haffty, B.G.; DiPaola, R.S.; Saunders, T.; Zloza, A.; Damare, S.; Beckett, Y.; Yu, B.; Najmi, S.; Gabel, C.; Dickerson, S.; Zheng, L.; El-Deiry, W.S.; Allen, J.E.; Stogniew, M.; Oster, W.; Mehnert, J.M. First-in-human clinical trial of oral ONC201 in patients with refractory solid tumors. *Clin. Cancer Res.,* **2017**, *23*(15), 4163-4169. http://dx.doi.org/10.1158/1078-0432.CCR-16-2658 PMID: 28331050

[42] Stein, M.N.; Malhotra, J.; Tarapore, R.S.; Malhotra, U.; Silk, A.W.; Chan, N.; Rodriguez, L.; Aisner, J.; Aiken, R.D.; Mayer, T.; Haffty, B.G.; Newman, J.H.; Aspromonte, S.M.; Bommareddy, P.K.; Estupinian, R.; Chesson, C.B.; Sadimin, E.T.; Li, S.; Medina, D.J.; Saunders, T.; Frankel, M.; Kareddula, A.; Damare, S.; Wesolowsky, E.; Gabel, C.; El-Deiry, W.S.; Prabhu, V.V.; Allen, J.E.; Stogniew, M.; Oster, W.; Bertino, J.R.; Libutti, S.K.; Mehnert, J.M.; Zloza, A. Safety and enhanced immunostimulatory activity of the DRD2 antagonist ONC201 in advanced solid tumor patients with weekly oral administration. *J. Immunother. Cancer,* **2019**, *7*(1), 136. http://dx.doi.org/10.1186/s40425-019-0599-8 PMID: 31118108

[43] Arrillaga-Romany, I.; Chi, A.S.; Allen, J.E.; Oster, W.; Wen, P.Y.; Batchelor, T.T. A phase 2 study of the first imipridone ONC201, a selective DRD2 antagonist for oncology, administered every three weeks in recurrent glioblastoma. *Oncotarget,* **2017**, *8*(45), 79298-79304. http://dx.doi.org/10.18632/oncotarget.17837 PMID: 29108308

[44] Hall, M.D.; Odia, Y.; Allen, J.E.; Tarapore, R.; Khatib, Z.; Niazi, T.N.; Daghistani, D.; Schalop, L.; Chi, A.S.; Oster, W.; Mehta, M.P. First clinical experience with DRD2/3 antagonist ONC201 in H3 K27M-mutant pediatric diffuse intrinsic pontine glioma: a case report. *J. Neurosurg. Pediatr.,* **2019**, *23*(6), 1-7. http://dx.doi.org/10.3171/2019.2.PEDS18480 PMID: 30952114

[45] Chi, A.S.; Tarapore, R.S.; Hall, M.D.; Shonka, N.; Gardner, S.; Umemura, Y.; Sumrall, A.; Khatib, Z.; Mueller, S.; Kline, C.; Zaky, W.; Khatua, S.; Weathers, S.-P.; Odia, Y.; Niazi, T.N.; Daghistani, D.; Cherrick, I.; Korones, D.; Karajannis, M.A.; Kong, X.-T.; Minturn, J.; Waanders, A.; Arillaga-Romany, I.; Batchelor, T.; Wen, P.Y.; Merdinger, K.; Schalop, L.; Stogniew, M.; Allen, J.E.; Oster, W.; Mehta, M.P. Pediatric and adult H3 K27M-mutant diffuse midline glioma treated with the selective DRD_2 antagonist ONC201. *J. Neurooncol.,* **2019**, *145*(1), 97-105. http://dx.doi.org/10.1007/s11060-019-03271-3 PMID: 31456142

[46] Weissenrieder, J.S.; Neighbors, J.D.; Mailman, R.B.; Hohl, R.J. Cancer and the dopamine d_2 receptor: a pharmacologi-

cal perspective. *J. Pharmacol. Exp. Ther.,* **2019**, *370*(1), 111-126.
http://dx.doi.org/10.1124/jpet.119.256818 PMID: 31000578

[47] Wang, S.; Che, T.; Levit, A.; Shoichet, B.K.; Wacker, D.; Roth, B.L. Structure of the D_2 dopamine receptor bound to the atypical antipsychotic drug risperidone. *Nature,* **2018**, *555*(7695), 269-273.
http://dx.doi.org/10.1038/nature25758 PMID: 29466326

[48] *Oncoceutics, ONC201, Briefing Document, Oncologic Drugs Advisory Committee Pediatric Subcommittee,* **2019**.
https://www.fda.gov/media/128027/download

[49] Ishizawa, J.; Zarabi, S.F.; Davis, R.E.; Halgas, O.; Nii, T.; Jitkova, Y.; Zhao, R.; St-Germain, J.; Heese, L.E.; Egan, G.; Ruvolo, V.R.; Barghout, S.H.; Nishida, Y.; Hurren, R.; Ma, W.; Gronda, M.; Link, T.; Wong, K.; Mabanglo, M.; Kojima, K.; Borthakur, G.; MacLean, N.; Ma, M.C.J.; Leber, A.B.; Minden, M.D.; Houry, W.; Kantarjian, H.; Stogniew, M.; Raught, B.; Pai, E.F.; Schimmer, A.D.; Andreeff, M. Mitochondrial ClpP-mediated proteolysis induces selective cancer cell lethality. *Cancer Cell,* **2019**, *35*(5), 721-737.e9.
http://dx.doi.org/10.1016/j.ccell.2019.03.014 PMID: 31056398

[50] Wang, S.; Dougan, D.A. The direct molecular target for Imipridone ONC201 is finally established. *Cancer Cell,* **2019**, *35*(5), 707-708.
http://dx.doi.org/10.1016/j.ccell.2019.04.010 PMID: 31085171

[51] Wong, K.S.; Houry, W.A. Chemical modulation of human mitochondrial ClpP: potential application in cancer therapeutics. *ACS Chem. Biol.,* **2019**, *14*(11), 2349-2360.
http://dx.doi.org/10.1021/acschembio.9b00347 PMID: 31241890

[52] Amor, A.J.; Schmitz, K.R.; Baker, T.A.; Sauer, R.T. Roles of the ClpX IGF loops in ClpP association, dissociation, and protein degradation. *Protein Sci.,* **2019**, *28*(4), 756-765.
http://dx.doi.org/10.1002/pro.3590 PMID: 30767302

[53] Pustylnikov, S.; Costabile, F.; Beghi, S.; Facciabene, A. Targeting mitochondria in cancer: current concepts and immunotherapy approaches. *Transl. Res.,* **2018**, *202*, 35-51.
http://dx.doi.org/10.1016/j.trsl.2018.07.013 PMID: 30144423

[54] Seo, J.H.; Rivadeneira, D.B.; Caino, M.C.; Chae, Y.C.; Speicher, D.W.; Tang, H.Y.; Vaira, V.; Bosari, S.; Palleschi, A.; Rampini, P.; Kossenkov, A.V.; Languino, L.R.; Altieri, D.C. The mitochondrial unfoldase-peptidase complex ClpXP controls bioenergetics stress and metastasis. *PLoS Biol.,* **2016**, *14*(7), e1002507.
http://dx.doi.org/10.1371/journal.pbio.1002507 PMID: 27389535

[55] Wong, K.S.; Houry, W.A. Recent advances in targeting human mitochondrial. *Mitochondria in Health and in Sickness*; Urbani, A.; Babu, M., Eds.; Springer Nature Singapore Pte. Ltd., **2019**, pp. 119-142.
http://dx.doi.org/10.1007/978-981-13-8367-0_8

[56] Moreno-Cinos, C.; Goossens, K.; Salado, I.G.; Van Der Veken, P.; De Winter, H.; Augustyns, K.; Clp, P. ClpP protease, a promising antimicrobial target. *Int. J. Mol. Sci.,* **2019**, *20*(9), 2232.
http://dx.doi.org/10.3390/ijms20092232 PMID: 31067645

[57] Zeiler, E.; Korotkov, V.S.; Lorenz-Baath, K.; Böttcher, T.; Sieber, S.A. Development and characterization of improved β-lactone-based anti-virulence drugs targeting ClpP. *Bioorg. Med. Chem.,* **2012**, *20*(2), 583-591.
http://dx.doi.org/10.1016/j.bmc.2011.07.047 PMID: 21855356

[58] Brötz-Oesterhelt, H.; Beyer, D.; Kroll, H.P.; Endermann, R.; Ladel, C.; Schroeder, W.; Hinzen, B.; Raddatz, S.; Paulsen, H.; Henninger, K.; Bandow, J.E.; Sahl, H.-G.; Labischinski, H. Dysregulation of bacterial proteolytic machinery by a new class of antibiotics. *Nat. Med.,* **2005**, *11*(10), 1082-1087.
http://dx.doi.org/10.1038/nm1306 PMID: 16200071

[59] Ye, F.; Li, J.; Yang, C.G. The development of small-molecule modulators for ClpP protease activity. *Mol. Biosyst.,* **2016**, *13*(1), 23-31.
http://dx.doi.org/10.1039/C6MB00644B PMID: 27831584

[60] Socha, A.M.; Tan, N.Y.; LaPlante, K.L.; Sello, J.K. Diversity-oriented synthesis of cyclic acyldepsipeptides leads to the discovery of a potent antibacterial agent. *Bioorg. Med. Chem.,* **2010**, *18*(20), 7193-7202.
http://dx.doi.org/10.1016/j.bmc.2010.08.032 PMID: 20833054

[61] Stahl, M.; Korotkov, V.S.; Balogh, D.; Kick, L.M.; Gersch, M.; Pahl, A.; Kielkowski, P.; Richter, K.; Schneider, S.; Sieber, S.A. Selective activation of human caseinolytic protease P (ClpP). *Angew. Chem. Int. Ed. Engl.,* **2018**, *57*(44), 14602-14607.
http://dx.doi.org/10.1002/anie.201808189 PMID: 30129683

[62] Stein, M.N.; Mayer, T.M.; Moss, R.A. Silk, A.W.; Chan, N.; Haffty, B.G.; DiPaola, R.S.; Beckett, Y.; Bentlyewski, E.; Zheng, L.; Fang, B.; Allen, J.E.; Mehnert, J.M. First-in-human dose escalation study of oral ONC201 in advanced solid tumors. *J. Clin. Oncol.,* **2015**, *33*(15_suppl), TPS2623-TPS2623.
http://dx.doi.org/10.1200/jco.2015.33.15_suppl.tps2623

[63] Graves, P.R.; Aponte-Collazo, L.J.; Fennell, E.M.J.; Graves, A.C.; Hale, A.E.; Dicheva, N.; Herring, L.E.; Gilbert, T.S.K.; East, M.P.; McDonald, I.M.; Lockett, M.R.; Ashamalla, H.; Moorman, N.J.; Karanewsky, D.S.; Iwanowicz, E.J.; Holmuhamedov, E.; Graves, L.M. Mitochondrial protease ClpP is a target for the anticancer compounds ONC201 and related analogues. *ACS Chem. Biol.,* **2019**, *14*(5), 1020-1029.
http://dx.doi.org/10.1021/acschembio.9b00222 PMID: 31021596

[64] Wagner, J.; Kline, C.L.; Ralff, M.D.; Lev, A.; Lulla, A.; Zhou, L.; Olson, G.L.; Nallaganchu, B.R.; Benes, C.H.; Allen, J.E.; Prabhu, V.V.; Stogniew, M.; Oster, W.; El-Deiry, W.S. Preclinical evaluation of the imipridone family, analogs of clinical stage anti-cancer small molecule ONC201, reveals potent anti-cancer effects of ONC212. *Cell Cycle,* **2017**, *16*(19), 1790-1799.
http://dx.doi.org/10.1080/15384101.2017.1325046 PMID: 28489985

[65] Jacob, N.T.; Lockner, J.W.; Kravchenko, V.V.; Janda, K.D. Pharmacophore reassignment for induction of the immunosurveillance cytokine TRAIL. *Angew. Chem. Int. Ed. Engl.,* **2014**, *53*(26), 6628-6631.
http://dx.doi.org/10.1002/anie.201402133 PMID: 24838721

[66] Ma, Z.; Gao, G.; Fang, K.; Sun, H. Development of novel anticancer agents with a scaffold of tetrahydropyrido[4,3-*d*]pyrimidine-2,4-dione. *ACS Med. Chem. Lett.,* **2019**, *10*(2), 191-195.
http://dx.doi.org/10.1021/acsmedchemlett.8b00531 PMID: 30783502

[67] Xu, R.L.Y. Imidazo-pyrimidine compounds, and preparation methods and application thereof. International Patent WO2016/184437, **2016**.

[68] Iwanowicz, E.J. Protein kinase regulators. International Patent WO2018/0319872018, **2018**.

[69] Iwanowicz, E.J. Protein kinase regulators. International Patent WO2018/031990A1, **2018**.

[70] Allen, J.E.; Prabhu, V.V.; Stogniew, M. Imipridones for Gliomas US. Patent US2020/0022982, **2020**.

[71] Kang, S.G.; Maurizi, M.R.; Thompson, M.; Mueser, T.; Ahvazi, B. Crystallography and mutagenesis point to an essential role for the N-terminus of human mitochondrial ClpP. *J. Struct. Biol.,* **2004**, *148*(3), 338-352. http://dx.doi.org/10.1016/j.jsb.2004.07.004 PMID: 15522782

[72] Wong, K.S.; Mabanglo, M.F.; Seraphim, T.V.; Mollica, A.; Mao, Y.Q.; Rizzolo, K.; Leung, E.; Moutaoufik, M.T.; Hoell, L.; Phanse, S.; Goodreid, J.; Barbosa, L.R.S.; Ramos, C.H.I.; Babu, M.; Mennella, V.; Batey, R.A.; Schimmer, A.D.; Houry, W.A. Acyldepsipeptide analogs dysregulate human mitochondrial ClpP protease activity and cause apoptotic cell death. *Cell Chem. Biol.,* **2018**, *25*(8), 1017-1030.e9. http://dx.doi.org/10.1016/j.chembiol.2018.05.014 PMID: 30126533

[73] Greenberger, J.S.; Cassady, J.R.; Levene, M.B. Radiation therapy of thalamic, midbrain and brain stem gliomas. *Radiology,* **1977**, *122*(2), 463-468. http://dx.doi.org/10.1148/122.2.463 PMID: 402018

[74] Halperin, E.C. Pediatric brain stem tumors: patterns of treatment failure and their implications for radiotherapy. *Int. J. Radiat. Oncol. Biol. Phys.,* **1985**, *11*(7), 1293-1298. http://dx.doi.org/10.1016/0360-3016(85)90244-5 PMID: 2989230

[75] Packer, R.J.; Boyett, J.M.; Zimmerman, R.A.; Albright, A.L.; Kaplan, A.M.; Rorke, L.B.; Selch, M.T.; Cherlow, J.M.; Finlay, J.L.; Wara, W.M. Outcome of children with brain stem gliomas after treatment with 7800 cGy of hyperfractionated radiotherapy. A Childrens Cancer Group Phase I/II Trial. *Cancer,* **1994**, *74*(6), 1827-1834. http://dx.doi.org/10.1002/1097-0142(19940915)74:6<1827::AID-CNCR2820740628>3.0.CO;2-Q PMID: 8082086

[76] Zaghloul, M.S.; Eldebawy, E.; Ahmed, S.; Mousa, A.G.; Amin, A.; Refaat, A.; Zaky, I.; Elkhateeb, N.; Sabry, M. Hypofractionated conformal radiotherapy for pediatric diffuse intrinsic pontine glioma (DIPG): a randomized controlled trial. *Radiother. Oncol.,* **2014**, *111*(1), 35-40. http://dx.doi.org/10.1016/j.radonc.2014.01.013 PMID: 24560760

[77] Janssens, G.O.; Gandola, L.; Bolle, S.; Mandeville, H.; Ramos-Albiac, M.; van Beek, K.; Benghiat, H.; Hoeben, B.; Morales La Madrid, A.; Kortmann, R.D.; Hargrave, D.; Menten, J.; Pecori, E.; Biassoni, V.; von Bueren, A.O.; van Vuurden, D.G.; Massimino, M.; Sturm, D.; Peters, M.; Kramm, C.M. Survival benefit for patients with diffuse intrinsic pontine glioma (DIPG) undergoing re-irradiation at first progression: a matched-cohort analysis on behalf of the SIOP-E-HGG/DIPG working group. *Eur. J. Cancer,* **2017**, *73*, 38-47. http://dx.doi.org/10.1016/j.ejca.2016.12.007 PMID: 28161497

[78] Lassaletta, A.; Strother, D.; Laperriere, N.; Hukin, J.; Vanan, M.I.; Goddard, K.; Lafay-Cousin, L.; Johnston, D.L.; Zelcer, S.; Zapotocky, M.; Rajagopal, R.; Ramaswamy, V.; Hawkins, C.; Tabori, U.; Huang, A.; Bartels, U.; Bouffet, E. Reirradiation in patients with diffuse intrinsic pontine gliomas: the Canadian experience. *Pediatr. Blood Cancer,* **2018**, *65*(6), e26988. http://dx.doi.org/10.1002/pbc.26988 PMID: 29369515

[79] Freeman, C.R.; Kepner, J.; Kun, L.E.; Sanford, R.A.; Kadota, R.; Mandell, L.; Friedman, H. A detrimental effect of a combined chemotherapy-radiotherapy approach in children with diffuse intrinsic brain stem gliomas? *Int. J. Radiat. Oncol. Biol. Phys.,* **2000**, *47*(3), 561-564. http://dx.doi.org/10.1016/S0360-3016(00)00471-5 PMID: 10837936

[80] Kilburn, L.B.; Kocak, M.; Baxter, P.; Poussaint, T.Y.; Paulino, A.C.; McIntyre, C.; Lemenuel-Diot, A.; Lopez-Diaz, C.; Kun, L.; Chintagumpala, M.; Su, J.M.; Broniscer, A.; Baker, J.N.; Hwang, E.I.; Fouladi, M.; Boyett, J.M.; Blaney, S.M. A pediatric brain tumor consortium phase II trial of capecitabine rapidly disintegrating tablets with concomitant radiation therapy in children with newly diagnosed diffuse intrinsic pontine gliomas. *Pediatr. Blood Cancer,* **2018**, *65*(2), 10.1002/pbc.26832. http://dx.doi.org/10.1002/pbc.26832 PMID: 29090526

[81] Cohen, K.J.; Heideman, R.L.; Zhou, T.; Holmes, E.J.; Lavey, R.S.; Bouffet, E.; Pollack, I.F. Temozolomide in the treatment of children with newly diagnosed diffuse intrinsic pontine gliomas: a report from the Children's Oncology Group. *Neuro-oncol.,* **2011**, *13*(4), 410-416. http://dx.doi.org/10.1093/neuonc/noq205 PMID: 21345842

[82] Chassot, A.; Canale, S.; Varlet, P.; Puget, S.; Roujeau, T.; Negretti, L.; Dhermain, F.; Rialland, X.; Raquin, M.A.; Grill, J.; Dufour, C. Radiotherapy with concurrent and adjuvant temozolomide in children with newly diagnosed diffuse intrinsic pontine glioma. *J. Neurooncol.,* **2012**, *106*(2), 399-407. http://dx.doi.org/10.1007/s11060-011-0681-7 PMID: 21858607

[83] Rizzo, D.; Scalzone, M.; Ruggiero, A.; Maurizi, P.; Attinà, G.; Mastrangelo, S.; Lazzareschi, I.; Ridola, V.; Colosimo, C.; Caldarelli, M.; Balducci, M.; Riccardi, R. Temozolomide in the treatment of newly diagnosed diffuse brainstem glioma in children: a broken promise? *J. Chemother.,* **2015**, *27*(2), 106-110. http://dx.doi.org/10.1179/1973947814Y.0000000228 PMID: 25466729

[84] Haas-Kogan, D.A.; Banerjee, A.; Poussaint, T.Y.; Kocak, M.; Prados, M.D.; Geyer, J.R.; Fouladi, M.; Broniscer, A.; Minturn, J.E.; Pollack, I.F.; Packer, R.J.; Boyett, J.M.; Kun, L.E. Phase II trial of tipifarnib and radiation in children with newly diagnosed diffuse intrinsic pontine gliomas. *Neuro-oncol.,* **2011**, *13*(3), 298-306. http://dx.doi.org/10.1093/neuonc/noq202 PMID: 21339191

[85] Pollack, I.F.; Jakacki, R.I.; Blaney, S.M.; Hancock, M.L.; Kieran, M.W.; Phillips, P.; Kun, L.E.; Friedman, H.; Packer, R.; Banerjee, A.; Geyer, J.R.; Goldman, S.; Poussaint, T.Y.; Krasin, M.J.; Wang, Y.; Hayes, M.; Murgo, A.; Weiner, S.; Boyett, J.M. Phase I trial of imatinib in children with newly diagnosed brainstem and recurrent malignant gliomas: a Pediatric Brain Tumor Consortium report. *Neuro-oncol.,* **2007**, *9*(2), 145-160. http://dx.doi.org/10.1215/15228517-2006-031 PMID: 17293590

[86] Jenkin, R.D.; Boesel, C.; Ertel, I.; Evans, A.; Hittle, R.; Ortega, J.; Sposto, R.; Wara, W.; Wilson, C.; Anderson, J. Brain-stem tumors in childhood: a prospective randomized trial of irradiation with and without adjuvant CCNU, VCR, and prednisone. A report of the Childrens Cancer Study Group. *J. Neurosurg.,* **1987**, *66*(2), 227-233. http://dx.doi.org/10.3171/jns.1987.66.2.0227 PMID: 3806204

[87] Jennings, M.T.; Sposto, R.; Boyett, J.M.; Vezina, L.G.; Holmes, E.; Berger, M.S.; Bruggers, C.S.; Bruner, J.M.; Chan, K.W.; Dusenbery, K.E.; Ettinger, L.J.; Fitz, C.R.; Lafond, D.; Mandelbaum, D.E.; Massey, V.; McGuire, W.;

McNeely, L.; Moulton, T.; Pollack, I.F.; Shen, V. Preradiation chemotherapy in primary high-risk brainstem tumors: phase II study CCG-9941 of the Children's Cancer Group. *J. Clin. Oncol.,* **2002**, *20*(16), 3431-3437. http://dx.doi.org/10.1200/JCO.2002.04.109 PMID: 12177103

[88] Ruggiero, A.; Rizzo, D.; Attinà, G.; Lazzareschi, I.; Maurizi, P.; Ridola, V.; Mastrangelo, S.; Migliorati, R.; Bertolini, P.; Colosimo, C.; Riccardi, R. Phase I study of temozolomide combined with oral etoposide in children with malignant glial tumors. *J. Neurooncol.,* **2013**, *113*(3), 513-518. http://dx.doi.org/10.1007/s11060-013-1145-z PMID: 23666235

[89] Jansen, M.H.; van Vuurden, D.G.; Vandertop, W.P.; Kaspers, G.J. Diffuse intrinsic pontine gliomas: a systematic update on clinical trials and biology. *Cancer Treat. Rev.,* **2012**, *38*(1), 27-35. http://dx.doi.org/10.1016/j.ctrv.2011.06.007 PMID: 21764221

[90] Ho, S.L.; Singh, R.; Zhou, Z.; Lavi, E.; Souweidane, M.M. Toxicity evaluation of prolonged convection-enhanced delivery of small-molecule kinase inhibitors in naïve rat brainstem. *Childs Nerv. Syst.,* **2015**, *31*(2), 221-226. http://dx.doi.org/10.1007/s00381-014-2568-3 PMID: 25269544

[91] Luther, N.; Cheung, N.K.; Souliopoulos, E.P.; Karampelas, I.; Bassiri, D.; Edgar, M.A.; Guo, H.F.; Pastan, I.; Gutin, P.H.; Souweidane, M.M. Interstitial infusion of glioma-targeted recombinant immunotoxin 8H9scFv-PE38. *Mol. Cancer Ther.,* **2010**, *9*(4), 1039-1046. http://dx.doi.org/10.1158/1535-7163.MCT-09-0996 PMID: 20371725

[92] Souweidane, M.M.; Occhiogrosso, G.; Mark, E.B.; Edgar, M.A. Interstitial infusion of IL13-PE38QQR in the rat brain stem. *J. Neurooncol.,* **2004**, *67*(3), 287-293. http://dx.doi.org/10.1023/B:NEON.0000024219.47447.91 PMID: 15164984

[93] Grasso, C.S.; Tang, Y.; Truffaux, N.; Berlow, N.E.; Liu, L.; Debily, M.A.; Quist, M.J.; Davis, L.E.; Huang, E.C.; Woo, P.J.; Ponnuswami, A.; Chen, S.; Johung, T.B.; Sun, W.; Kogiso, M.; Du, Y.; Qi, L.; Huang, Y.; Hütt-Cabezas, M.; Warren, K.E.; Le Dret, L.; Meltzer, P.S.; Mao, H.; Quezado, M.; van Vuurden, D.G.; Abraham, J.; Fouladi, M.; Svalina, M.N.; Wang, N.; Hawkins, C.; Nazarian, J.; Alonso, M.M.; Raabe, E.H.; Hulleman, E.; Spellman, P.T.; Li, X.N.; Keller, C.; Pal, R.; Grill, J.; Monje, M. Functionally defined therapeutic targets in diffuse intrinsic pontine glioma. *Nat. Med.,* **2015**, *21*(6), 555-559. http://dx.doi.org/10.1038/nm.3855 PMID: 25939062

[94] Pollack, I.F.; Stewart, C.F.; Kocak, M.; Poussaint, T.Y.; Broniscer, A.; Banerjee, A.; Douglas, J.G.; Kun, L.E.; Boyett, J.M.; Geyer, J.R. A phase II study of gefitinib and irradiation in children with newly diagnosed brainstem gliomas: a report from the Pediatric Brain Tumor Consortium. *Neuro-oncol.,* **2011**, *13*(3), 290-297. http://dx.doi.org/10.1093/neuonc/noq199 PMID: 21292687

[95] Van Gool, S.W.; Makalowski, J.; Bonner, E.R.; Feyen, O.; Domogalla, M.P.; Prix, L.; Schirrmacher, V.; Nazarian, J.; Stuecker, W. Addition of Multimodal Immunotherapy to Combination Treatment Strategies for Children with DIPG: A Single Institution Experience. *Medicines (Basel),* **2020**, *7*(5), 29-45. http://dx.doi.org/10.3390/medicines7050029 PMID: 32438648

[96] Ensan, D.; Smil, D.; Zepeda-Velázquez, C.A.; Panagopoulos, D.; Wong, J.F.; Williams, E.P.; Adamson, R.; Bullock, A.N.; Kiyota, T.; Aman, A.; Roberts, O.G.; Edwards, A.M.; O'Meara, J.A.; Isaac, M.B.; Al-Awar, R. Targeting ALK2: an open science approach to developing therapeutics for the treatment of diffuse intrinsic pontine glioma. *J. Med. Chem.,* **2020**, *63*(9), 4978-4996. http://dx.doi.org/10.1021/acs.jmedchem.0c00395 PMID: 32369358

[97] Bailey, C.P.; Figueroa, M.; Gangadharan, A.; Yang, Y.; Romero, M.M.; Kennis, B.A.; Yadavilli, S.; Henry, V.; Collier, T.; Monje, M.; Lee, D.A.; Wang, L.; Nazarian, J.; Gopalakrishnan, V.; Zaky, W.; Becher, O.J.; Chandra, J. Pharmacologic inhibition of lysine specific demethylase-1 (LSD1) as a therapeutic and immune-sensitization strategy in pediatric high grade glioma (pHGG). *Neuro-oncol.,* **2020**, *22*(9), 1302-1314. https://doi.org/10.1093/neuonc/noaa058 PMID: 32166329

[98] Ralff, M.D.; Lulla, A.R.; Wagner, J.; El-Deiry, W.S. ONC201: a new treatment option being tested clinically for recurrent glioblastoma. *Transl. Cancer Res.,* **2017**, *6*(Suppl. 7), S1239-S1243. http://dx.doi.org/10.21037/tcr.2017.10.03 PMID: 30175049